THE JOURNAL OF BIOLOGICAL CHEMISTRY VOL. 289, NO. 24, pp. 17054–17069, June 13, 2014

The Phytoestrogen Genistein Modulates Lysosomal Metabolism and Transcription Factor EB (TFEB) Activation*

Received for publication, February 4, 2014, and in revised form, April 24, 2014 Published, JBC Papers in Press, April 25, 2014, DOI 10.1074/jbc.M114.555300

Marta Moskot[‡], Sandro Montefusco[§], Joanna Jakóbkiewicz-Banecka[¶], Paweł Mozolewski[¶], Alicja Węgrzyn[‖], Diego Di Bernardo[§], Grzegorz Węgrzyn[¶], Diego L. Medina[§1], Andrea Ballabio[§‡‡§§], and Magdalena Gabig-Cimińska[‡2]**

*From the [‡]Laboratory of Molecular Biology (affiliated with the University of Gdańsk), Institute of Biochemistry and Biophysics, Polish Academy of Sciences, Wita Stwosza 59, 80-308 Gdańsk, Poland, the [§]High Content Screening Facility, Telethon Institute of Genetics and Medicine (TIGEM), Via P. Castellino 111, 80131 Naples, Italy, the [¶]Department of Molecular Biology, University of Gdańsk, Wita Stwosza 59, 80-308 Gdańsk, Poland, the [‖]Department of Microbiology, University of Szczecin, Felczaka 3c, 71-412 Szczecin, Szczecin, Poland, the **Department of Molecular and Human Genetics, Baylor College of Medicine, Houston, Texas 77030, the [‡‡]Jan and Dan Duncan Neurological Research Institute, Texas Children's Hospital, Houston, Texas 77030, and [§§]Medical Genetics, Department of Pediatrics, Federico II University, Via Pansini 5, 80131 Naples, Italy*

Background: Genistein is a potential drug for certain inherited lysosomal disorders.
Results: Genistein influences molecular cross-talk in the cell responsible for lysosomal enhancement.
Conclusion: Genistein potentiates lysosomal metabolism by activating transcription factor EB (TFEB).
Significance: The explanation of genistein action offers more adequate therapeutic procedures for the treatment of some lysosomal storage diseases.

Genistein (5,7-dihydroxy-3-(4-hydroxyphenyl)-4H-1-benzopyran-4-one) has been previously proposed as a potential drug for use in substrate reduction therapy for mucopolysaccharidoses, a group of inherited metabolic diseases caused by mutations leading to inefficient degradation of glycosaminoglycans (GAGs) in lysosomes. It was demonstrated that this isoflavone can cross the blood-brain barrier, making it an especially desirable potential drug for the treatment of neurological symptoms present in most lysosomal storage diseases. So far, no comprehensive genomic analyses have been performed to elucidate the molecular mechanisms underlying the effect elicited by genistein. Therefore, the aim of this work was to identify the genistein-modulated gene network regulating GAG biosynthesis and degradation, taking into consideration the entire lysosomal metabolism. Our analyses identified over 60 genes with known roles in lysosomal biogenesis and/or function whose expression was enhanced by genistein. Moreover, 19 genes whose products are involved in both GAG synthesis and degradation pathways were found to be remarkably differentially regulated by genistein treatment. We found a regulatory network linking genistein-mediated control of transcription factor EB (TFEB) gene expression, TFEB nuclear translocation, and activation of TFEB-dependent lysosome biogenesis to lysosomal metabolism. Our data indicate that the molecular mechanism of genistein action involves not only impairment of GAG synthesis but more importantly lysosomal enhancement via TFEB. These findings contribute to explaining the beneficial effects of genistein in lysosomal storage diseases as well as envisage new therapeutic approaches to treat these devastating diseases.

Lysosomal storage diseases are a group of over 50 rare inherited metabolic disorders that result from defects in lysosomal function (1), leading usually to deficiency of a single enzyme required for the metabolism of lipids, glycoproteins, or glycosaminoglycans. Alterations in metabolism of GAGs[3] due to mutations in genes coding for enzymes involved in degradation of these compounds cause severe inherited metabolic diseases called mucopolysaccharidoses (2). Impaired hydrolysis of GAGs leads to their accumulation in the patient's cells, which results in progressive damage of the affected tissues and organs, including the heart, respiratory system, bones, joints, and central nervous system (CNS).

Currently, bone marrow or hematopoietic stem cell transplantations (the latest one has been shown to be effective in MPS I, although no cure can be achieved) and enzyme replacement therapy are the only approved treatments of MPS. However, neurological symptoms, developing due to GAG accumulation in CNS, cannot be managed by enzyme replacement therapy due to an inefficient delivery of proteins through the blood-brain barrier (3). Although gene therapy is a promising hope for MPS patients, so far it remains a treatment under development rather than a real therapy (4). Therefore, there is still a need for alternative therapies, which could be helpful for patients suffering from mucopolysaccharidosis, especially from its neuropathic forms.

* This work was supported by National Science Centre Project Grants 2011/01/B/NZ1/03686 and N N301 668540 and was operated within the Foundation for Polish Science Team Programme co-financed by European Union European Regional Development Fund Grant TEAM/2008-2/7.
[1] To whom correspondence may be addressed. Tel.: 39-081-6132298; E-mail: medina@tigem.it.
[2] To whom correspondence may be addressed. Tel.: 48-58-523-6046; E-mail: m.gabig@biol.ug.edu.pl.

[3] The abbreviations used are: GAG, glycosaminoglycan; CLEAR, coordinated lysosomal expression and regulation; MPS, mucopolysaccharidosis; TFEB, transcription factor EB; HDFa, human dermal fibroblast(s); qRT-PCR, quantitative RT-PCR; GSEA, gene set enrichment analysis.

One potential therapeutic method for MPS is substrate reduction therapy (5). This kind of therapy is based on an assumption that inhibition of synthesis of compounds that cannot be efficiently degraded may facilitate an establishment of a new balance between their production and degradation, already lost due to a defect in a specific hydrolase (6). Previously, our group has demonstrated that genistein (5,7-dihydroxy-3-(4-hydroxyphenyl)-4H-1-benzopyran-4-one), a natural isoflavone, inhibited synthesis of glycosaminoglycans and reduced lysosomal GAG storage (7). It was demonstrated that this isoflavone can cross the blood-brain barrier, making it a desirable potential drug for the treatment of neuropathic forms of mucopolysaccharidoses. Importantly, genistein caused a marked improvement in treated mice suffering from MPS II and MPS IIIB diseases (8–10).

It has been shown that the primary mechanism of genistein-mediated inhibition of GAG synthesis involves epidermal growth factor (EGF), resulting in genistein affected EGF receptor-catalyzed phosphorylation efficiency (11). We hypothesized that this may lead to changes in expression of certain genes involved in glycosaminoglycan metabolism, and a potential substrate reduction therapy for MPS with the use of genistein has been called "gene expression-targeted isoflavone therapy," or GET IT. Therefore, the aim of this work was to identify the genistein-modulated gene network regulating GAG biosynthesis and degradation, taking into consideration the entire lysosomal metabolism.

EXPERIMENTAL PROCEDURES

Cell Cultures—Human dermal fibroblasts (HDFa) were obtained from Cascade Biologics, whereas mouse embryonic fibroblasts and HeLa cells were purchased from ATCC and cultured from cryo-preserved cells in Dulbecco's modified Eagle's medium (DMEM; Sigma-Aldrich) and Roswell Park Memorial Institute medium (RPMI 1640), respectively, with 10% fetal bovine serum (FBS) and 1% antibiotic/antimycotic solution (Sigma-Aldrich) and incubated at 5% CO_2 at 37 °C. For transcriptomic analyses, cells were seeded to a confluence of ~80%. After 24 h of growth, the medium was replaced with fresh non-supplemented medium (pure control K1), containing DMSO at a final concentration of 0.05% (vehicle control K2) or genistein at 30, 60, and 100 μM concentrations in 0.05% DMSO. The experimental treatment was carried out for 1-, 24-, and 48-h periods. These time course data sets and genistein doses were analyzed in the context of cell proliferation and cytotoxicity determined in previous studies (7).

RNA Extraction—Total RNA was extracted from cells using the High Pure RNA Isolation Kit (Roche Applied Science) and quantified with the Quant-it™ RiboGreen® assay kit (Invitrogen). In addition, the quality of each RNA sample was assessed using the RNA 6000 nanoassay on the Agilent 2100 Bioanalyzer (Agilent Technologies).

Microarray Assay Performance, Data Extraction, and Statistical Analysis—Three to five biological replicates (n) were conducted for the microarray analysis with the use of Illumina's Human HT-12 v3 and v4 Expression BeadChips (Illumina Inc.) for all tested conditions. The Illumina TotalPrep RNA amplification kit (Ambion) was used in order to amplify total input RNA. BeadChips were scanned using the Illumina BeadArray Reader and Bead Scan software (Illumina Inc.). The quality of microarray data was controlled by examining raw and adjusted intensity histograms. The detection scores (p values) were used to determine expressions of each gene after quantile normalization using the Illumina GenomeStudio software package (Gene Expression Module version 1.9.0, Illumina Inc.). All gene expression data have been deposited in the NCBI Gene Expression Omnibus (GEO series accession number GSE34074), according to the MIAME (minimum information about a microarray experiment) standards. An overview of experiment performance was gained by clustering samples using a correlation metric (Illumina® BeadStudio Data Analysis software). Average-linkage hierarchy was performed on the resulting gene set by using MultiExperimental Viewer version 4.8 (12). The Pearson correlation coefficient method was used to calculate "expression distance values" across experiments and to group samples that have similar expression patterns. The values ranging between 0.98 and 0.99 for biological replicates indicate a high degree of reproducibility and strong correspondences between expression profiles. Significantly differentially expressed genes had to have a -fold change greater than or equal to 2.0 or 1.3 and below 0.5 or 0.7 for whole genome or GAG-associated transcripts, respectively, with a p value of <0.05. In addition, GOrilla (gene ontology enrichment analysis and visualization tool) and gene set enrichment analysis (GSEA) were utilized (13, 14). Affected biological pathways were defined according to Kyoto Encyclopedia of Genes and Genomes annotation (15).

Genome Analysis—Human promoters were retrieved from the Ensemble database and analyzed with the CLEAR position weight matrix by using PatSer from the Regulatory Sequence Analysis Tool with default parameters. A score was assigned to each human promoter, equal to the PatSer score associated with sequences similar to the CLEAR position weight matrix. Gene Ontology analyses were performed with the GOrilla tool (13).

Real-time Quantitative RT-PCR—Real-time quantitative reverse transcription-PCR (real-time qRT-PCR) was performed to measure the mRNA levels of the studied genes using the LightCycler® System 480 (Roche Applied Science). Of the three so-called housekeeping gene candidates (*i.e. GAPDH*, *PBGD*, and *TBP*) exhibiting stable expression under our experimental conditions (based on the microarray data), probes for the latter two, bought from Roche Applied Science, were implemented for real-time qRT-PCR as reference genes because they appeared to be the best suited standards for the analysis (BestKeeper, an Excel-based software tool using pairwise correlations, was utilized (16)). mRNA from 0.5 μg of total input RNA was reverse-transcribed into cDNA using the Transcriptor First Strand cDNA synthesis kit (Roche Applied Science). Real-time qRT-PCR amplification was performed using the Universal Probe Library Set, Human, LightCycler® TaqMan® Master (Roche Applied Science), and the parameters used were according to the recommendations of Roche Applied Science. Primers obtained from Thermo Fisher Scientific GmbH and probes derived from Roche Applied Science used in the real-time qRT-PCR are presented in Table 1.

TABLE 1

Sequences and detailed information regarding primers and probes used for real-time quantitative RT-PCR validation of selected genes

TARGET		TRANSCRIPT	REFERENCE GENE	PRIMERS*	AMPLICON		PROBE
		Name/Length Sequence ID		Sequence/Length	Length (nt)	Region	
GAG BIOSYNTHESIS	CS	CHPF/3013 NM_024536.5	*GAPDH, TBP*	F: GGTCGCTGCATTCTCGAT/18 R: GGCACTTCGGAAATGAGG/18	126	exons 2-3 1062	# 36
		XYLT1/9336 NM_022166.3	*GAPDH, TBP*	F: GATATGAATTTCTTGAAGTCACACG/25 R: CAGGAAGAGCCGATCCAG/18	78	exons 5-6 1415	# 38
	HS	EXT1/3376 NM_000127.2	*GAPDH*	F: GCTTGGGTCCTTCAGATTCC/20 R: CATCCATTGCTGAGCATCAC/20	70	exons 2-3 1795	# 27
			TBP	F: AGCCCCTACCAGCCAAAC/18 R: GAAAACGGCTGCTCATAACC/20	90	exons 8-9 2335	# 59
		GLCE/5043 NM_015554.1	*GAPDH, TBP*	F: TGTCAAACAGTTTATTGCACCAG/23 R: TCCATTTGTCAAGAACTTGAGGT/23	106	exons 4-5 1035	# 48
		HS2ST1/6770 NM_012262.3	*GAPDH, TBP*	F: TGGCCATAGCTCCGAATG/18 R: TTAGGTTATACTTGGCTTGATCCAT/25	68	exons 5-6 1051	# 38
	KS	ST3GAL2/4450 NM_006927.3	*GAPDH,TBP*	F: GTCTGGACCCGAGAGAACAT/20 R: TGGTGTTGTGTGACTTGAACTG/22	88	exons 2-3 1429	# 77
GAG DEGRADATION	HS, KS	GNS/5144 NM_002076.3	*GAPDH, TBP*	F: GGGATGACTTTTTCCAGTGC/20 R: CGTGATGATTATGTGGGTACTTTC/24	92	exons 2-3 398	# 3
	KS	HEXA/2437 NM_000520.4	*GAPDH, TBP*	F: CCCCTGGCATTTGAAGGTA/19 R: ACATATTCTCCCCACATACAAGC/23	127	exons 12-13 1534	# 22
	DS, HS	IDUA/2203 NM_000203.3	*GAPDH, TBP*	F: GCTCAACCTCGCCTATGTG/19 R: TGGGTGAAGTTGTAGCTCCAGG/21	126	exons 2-3 301	# 66
	HS	NAGLU/2798 NM_000263.3	*GAPDH, TBP*	F: CCTCAGAGCCCTCCTACCTT/20 R: CTTGGAGCAGCCACACAG/18	63	exons 4-5 1329	# 86
		SGSH/2770 NM_000199.3	*GAPDH, TBP*	F: GGCACTGCTGAACCCTTACT/20 R: GGATCGAGAACCAATCCAAG/20	121	exons 7-8 952	# 57
OTHER		ARSG/2770 NM_014960.3	*GAPDH, TBP*	F: AAGCAACCCAGTTCATCCAG/20 R: GTGGGCCAGAGCCACATA/18	71	exons 6-7 1473	# 4
		ASAH1/2618 NM_177924.3	*GAPDH, TBP*	F: ACAGTTCTGGAAAATAGCACAAGT/25 R: GGTTGCCTCCCAGGATAAAG/20	98	exons 9-10 1074	# 57
		GBA/2324 NM_000157.3	*GAPDH, TBP*	F: CTTTGTCGACAGTCCCATCA/20 R: CCCTCAGGAATGAACTTGCT/20	102	exons 9-10 1471	# 9
		GM2A/3690 NM_000405.4	*GAPDH, TBP*	F: GTGTCCCCCTGAGTTCTCCT/20 R: GTCTGTGCATGGGATCTTGA/20	86	exons 2-3 384	# 10
		MAN2B1/3239 NM_001173498.1	*GAPDH,TBP*	F: GAGAGATGGCTCGCTGGA/18 R: TCCATTAGTGGCTCCGATACTC/22	72	exons 19-20 2985	# 66
		MANBA/3311 NM_005908.3	*GAPDH, TBP*	F: ACCAGACTGGGTACAACATGACT/23 R: AGTTCCACTGTCCTAAAATAAACCTT/26	94	exons 7-8 990	# 58
		SMPD1/2482 NM_000543.4	*GAPDH, TBP*	F: CTATGAAGCGATGGCCAAG/19 R: TGGGGAAAGAGCATAGAACC/20	91	exons 2-3 1214	# 71
		TFEB/2364 NM_007162.2	*GAPDH, TBP*	F: CTGCATGCGCAACCCTAT/18 R: CGGCAGTGCCTGGTACAT/18	71	exons 2-3 262	# 83
			HPRT	F: CAAGGCCAATGACCTGGAC/19 R: AACACCCTTTCCAAATCCTCA/21	105	Exons 6-7 1090	--
		CTSF/2032 NM_003793.3	*HPRT*	F: ACAGAGGAGGAGTTCCGCACTA/22 R: GCTTGCTTCATCTTGTTGCCA/21	74	Exons 9-10 808	--
		MCOLN1/2118 NM_020533.2	*HPRT*	F: GAGTCCCTGCGACAAGTTTC /20 R: TGTTCTCTTCCCGGAATGTC/20	143	Exons 2-3 291	--
		NEU1/2088 NM_000434.3	*HPRT*	F: TGAAGTGTTTGCCCCTGGAC/20 R: AGGCACCATGATCATCGCTG/20	137	Exons 3-4 735	--
		TPP1/3540 NM_000391.3	*HPRT*	F: GATCCCAGCTCTCCTCAATAC/21 R: GCCATTTTTGCACCGTGTG/19	99	Exons 3-4 269	--
		GAPDH/1338 NM_002046	reference gene	F: CTCTGCTCCTCCTGTTCGAC/20 R: GCCCAATACGACCAAATCC/19	119	exons 1-2-3 126	# GAPDH
		HPRT/1435 NM_000194.2	reference gene	F: TGGCGTCGTGATTAGTGATG R: AACACCCTTTCCAAATCCTCA	90	Exons 1-2 185	--
		TBP/1851 NM_003194	reference gene	F: TGAATCTTGGTTGTAAACTTGACC/24 R: CTCATGATTACCGCAGCAAA/20	94	exons 4-5 824	# TBP

siRNA Transfection—HeLa cells were seeded in triplicate into 12-well plates and cultured in RPMI 1640 medium with 10% FBS, 1% L-glutamine, and 1% penicillin/streptavidin solution (Sigma-Aldrich) at 5% CO_2 at 37 °C. After 24 h, cells were transfected with Lipofectamine RNAiMAX (Invitrogen) and 5 nM ON-TargetPlus Human TFEB siRNA-SMARTpool (Thermo Fisher Scientific) in Opti-MEM reduced serum medium (Invitrogen) according to the manufacturer's instructions. 72 h after transfection, the cells were processed for the indicated experimental procedures.

Immunoblotting—Cells were lysed, and the sample material was prepared as described previously (17). Protein concentration was determined with the BCA reagent (Thermo Scientific). Proteins were separated by 12% SDS-PAGE and immunoblotted onto a PVDF membrane (Millipore). The membrane was blocked for 5 h with 5% nonfat milk in PBS-T buffer (PBS with 0.05% Tween 20); incubated with primary antibodies anti-GAPDH (Sigma-Aldrich; 1:5000), anti-TFEB (Santa Cruz Biotechnology; 1:20), and anti-H4 (Santa Cruz Biotechnology; 1:100) at 4 °C overnight; washed three times with PBS-T buffer; and afterward incubated with horseradish peroxidase secondary antibody conjugate IgG (Sigma-Aldrich; 1:5000) at room temperature for 1 h and rinsed three times with PBS-T buffer for detection of expressed proteins using SuperSignal West Pico Chemiluminescent Substrate (Thermo Scientific) in a Fluor-S MultiImager (Bio-Rad).

Fluorescence Assays—TFEB-FLAG HeLa cells (18) were seeded on 96-well plates, incubated for 24 h, and treated with genistein ranging from 30 to 150 μM and 0.3 μM Torin 1 (Biomarin) in FBS-free medium. After 3 h at 37 °C, the cells were washed, fixed, and stained with 4′,6-diamidino-2-phenylindole (DAPI) (Sigma-Aldrich). For the acquisition of images, 10 pictures per well of the 96-well plate were taken by using confocal automated microscopy (Opera High Content Screening system, PerkinElmer Life Sciences). A dedicated script calculating the ratio value resulting from the average intensity of nuclear TFEB-GFP fluorescence divided by the average of the cytosolic intensity of TFEB-GFP fluorescence was developed to perform the analysis of TFEB localization on the different images (Acapella software, PerkinElmer Life Sciences). To visualize the acidophilic compartments of the cell, we used both acridine orange (19) and LysoTracker Red DN-99 (Molecular Probes, Invitrogen). Cells were incubated with 75 nM LysoTracker Red DN-99 for 1 h at 37 °C, rinsed with PBS, and fixed with 4% paraformaldehyde in PBS for 15 min at room temperature. Counterstaining was done with DAPI. Images were taken using a fluorescent microscope (Nikon Eclipse TE 300) with ×60 magnification.

High Content Screening Assay to Measure β-Galactosidase Expression—An HC assay that measures and quantifies β-galactosidase protein levels was developed at the high content screening facility (Telethon Institute of Genetics and Medicine) by using mouse embryonic fibroblasts isolated from a β-galactosidase knock-in mouse expressing the mentioned reporter gene in one allele of the TFEB locus (generated at the A. Ballabio laboratory). β-Gal-KI mouse embryonic fibroblasts were seeded on 96-well plates, incubated for 24 h, and treated with genistein ranging from 30 to 300 μM in a regular medium. After 24 h at 37 °C, cells were washed, fixed, and stained with antibodies against β-galactosidase (Abcam). For the acquisition of images, 10 pictures/well of the 96-well plate were taken by using confocal automated microscopy (Opera High Content Screening system; PerkinElmer Life Sciences). A dedicated script was developed to perform the analysis of β-galactosidase staining on the different images (Acapella software, PerkinElmer Life Sciences). The script calculates the average of fluorescence intensity per well. The results were normalized using negative (DMSO) control samples in the same plate. The dose-response curve and EC_{50} were calculated using Prism software.

TABLE 2

Number of genes whose expression was altered as a function of the treatment type identified in the microarray analysis among whole genome sequences and transcripts of HDFa cells associated with GAG metabolism ($n \geq 3$ experiments)

Significantly differentially expressed genes had a -fold change ≥2.0 or 1.3, and <0.5 or 0.7, for whole genome or GAG-associated transcripts, respectively, with a p value of <0.05. The cells responded to the different types of treatment with changes in gene expression profiling affecting a large number of genes. For genistein at 60 μM, the microarray analysis identified 259 genes that showed a significant increase or decrease over the 24-h time course, whereas 370 transcripts were expressively altered after 48 h, with 143 genes included in both sets. Treatment of cells with 100 μM genistein for 24 h affected 231 up- and 236 down-regulated transcripts, whereas the highest number of differentially expressed genes (291 increased and 370 decreased) was detected after 48 h.

Gene expression modulation	Modulation targets	No. of genes								
		Genistein concentration [μM]								
		30			60			100		
		Time of exposure [h]								
		1	24	48	1	24	48	1	24	48
▲ up-regulated genes	whole genome	7	12	25	1	110	155	6	231	291
	GAG metabolism	1	1	0	2	8	6	1	12	6
▼ down-regulated genes	whole genome	18	21	34	8	149	215	23	236	370
	GAG metabolism	0	0	0	0	4	1	1	4	3

RESULTS

Global Gene Expression Analysis Using Microarrays—Testing the effect of genistein on human fibroblast transcriptome, we found that this compound induced dose- and time-dependent alterations in transcript profiles in HDFa *in vitro* (Table 2). By carefully studying gene expression levels modulated after 24 h of treatment with 30, 60, and 100 μM genistein, we obtained 15 transcripts in common between all three doses (Fig. 1), whereas 37 transcripts after 48 h of genistein handling were affected, with seven genes (four up-regulated, *i.e. MAOA, MT1X, SLC40A1,* and *SCG5;* and three down-regulated, *i.e. CDCA8, RGS4,* and *TPX2*) modulated by genistein included in both the 24- and 48-h time course sets. Generally, at the top of the list of genistein-up- and down-regulated genes, there were those mainly involved in regulatory processes in the cell (Fig. 2). Detailed analysis showed a significant enhancement of expression for 64 genes with a known role in lysosomal biogenesis and/or function, among which nearly 50% are associated with lysosomal diseases in humans (Fig. 2, *A* and *B* (with a -fold change of at least 50%, $p < 0.001$) and Table 3 (with -fold change values from 1.3 to 2.9, $p < 0.01$)). For some of these genes, this was also confirmed by real-time qRT-PCR analysis (Fig. 3). Accordingly, GSEA showed a significant enrichment (enrichment score = 0.52; $p < 0.001$) of lysosome-related genes (Fig. 4).

Profiling of Expression of Genes Involved in Glycosaminoglycan Metabolism with Microarrays—Among 69 genes of glycosaminoglycan synthesis and degradation pathways (*i.e.* 14 genes in keratan sulfate biosynthesis, 23 in heparan sulfate biosynthe-

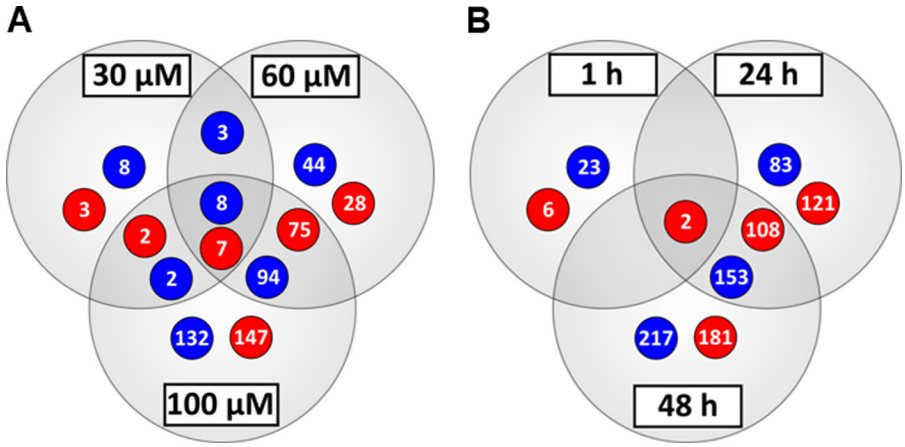

FIGURE 1. **Venn diagrams illustrating distribution of up-regulated (*black symbols*) and down-regulated (*white symbols*) genes of whole genome of HDFa cells after 24-h treatment with 30, 60, and 100 μM (*A*) or 1-, 24-, and 48-h treatment with 100 μM genistein (*B*).** The *digits inside* the *symbols* represent the numbers of transcripts identified as changed under studied conditions with corresponding overlap between the data sets. DMSO-treated cells were used in control experiments. Genistein made significant changes in gene expression in the cells at 60 and 100 μM final concentrations in the medium. Most time-dependent changes in gene expression occurred by 24 h for both genistein doses, with additional transcripts increasing and decreasing after that time.

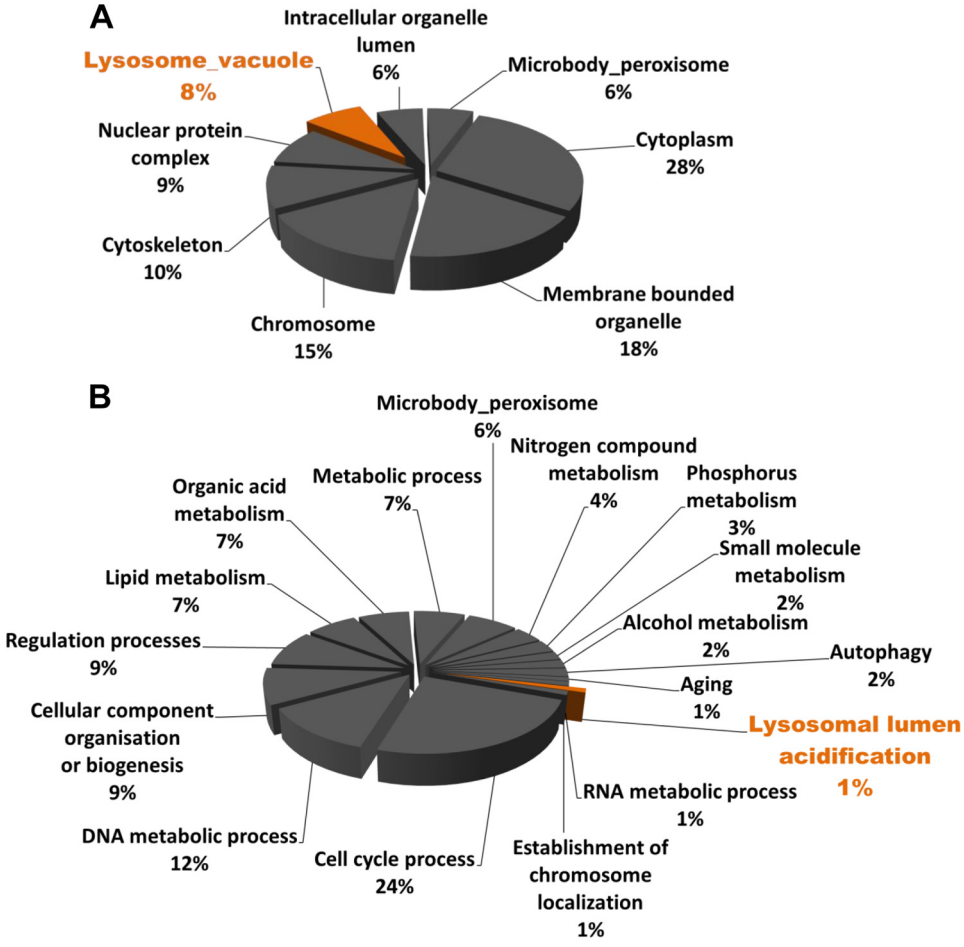

FIGURE 2. **Gene ontology analysis by "cellular compartment" (*A*) and "biological processes" (*B*) categories of the genes with expression modulated upon genistein treatment of HDFa cells, with false discovery rate <0.1, -fold change ≥1.3 and <0.7, and $p < 0.001$.**

sis, 21 in chondroitin/dermatan sulfate biosynthesis, and 18 in GAG degradation), including seven genes involved in more than one type of metabolic pathway, 19 genes in total were found to be remarkably differentially expressed in HDFa, as revealed by the microarray analysis. Among them, 12 genes involved in GAG biosynthesis pathways had modulated expression in 60 and 100 μM genistein-treated cells over a 24- and 48-h time course, with seven up-regulated (*i.e. CHPF*, *CHST7*, *CHST12*, *EXTL2*, *GLCE*, *HS2ST1*, and *NDST2*) and the other five (*i.e. CHST14*, *EXT1*, *HS3ST3A1*, *ST3GAL2*, and *XYLT1*) down-regulated by genistein. In addition, all seven genes associated with the GAG degradation pathway (*i.e. GNS*, *HEXA*,

TABLE 3

Selected genes with a known role in lysosomal biogenesis and/or function, also encoding enzymes of degradation pathways of organic compounds accumulated in the cells of patients with lysosomal storage disorder for which transcriptomic profiling with the use of DNA microarrays (24- and 48-h treatment with 100 μM genistein) and qRT-PCR (24-h treatment with 100 μM genistein) revealed increased expressions

Values represent -fold change ≥1.3 with S.D. (FC ± SD, $n \geq 3$) and denote significant differences for samples treated with genistein against untreated samples, with respect to *GAPDH* mRNA expression at a constant level. Distribution of CLEAR elements in the gene promoters is indicated.

Category	Enzyme	LSD or complication	Gene	Microarray FC ± SD		qRT-PCR*	CLEAR element	Position**
				24 h	48 h	24 h		
Lysosomal acid hydrolases and accessory proteins	acid phosphatase 2	Acid phosphatase deficiency	*ACP2*	1.5 ± 0.2	1.2 ± 0.2	n.d.	ACCTCAGGTGATCT	**-973**
	acid phosphatase 5	Unknown	*ACP5*	1.6 ± 0.1	1.8 ± 0.6	n.d.	AGATCACCTGAGAT GTGCCACGTGAGAA GGCTCACCTGGGTC GGCTCACATGACCC GGCTCACCTGGGTC	**-900** **-442** **-202** **-25** **9**
	aspartylglucosaminidase	Aspartylglucosoaminuria	*AGA*	1.9 ± 0.5	2.3 ± 0.2	n.d.	-	-
	arylsulfatase A	Metachromatic leukodystrophy	*ARSA*	1.3 ± 0.2	1.5 ± 0.2	n.d.	GCGCCAAGTGACTT	**106**
	arylsulfatase G	Unknown	*ARSG*	1.2 ± 0.4	1.8 ± 0.5	2.3 ± 0.4	GTCCCACGTGGACC TGCGCGCGTGACCC GAGCCACGTGTGCC	**6** **170** **184**
	acid ceramidase 1	Farber lipogranulomatosis	*ASAH1*	1.7 ± 0.8	1.5 ± 0.3	2.5 ± 0.2	CGCCCACCTGAGTC CGCCCACCTGAGTC	**-476** **154**
	cathepsin A	Galactosialidosis	*CTSA*	1.6 ± 0.3	1.6 ± 0.3	n.d.	AGGCCAGCTGGCGC	**59**
	cathepsin B	Unknown	*CTSB*	1.3 ± 0.2	1.3 ± 0.2	n.d.	ACCTCAGGTGACTC TGGTCACGTGGGGC	**-899** **-8**
	cathepsin D	Unknown	*CTSD*	1.2 ± 0.4	1.9 ± 0.4	n.d.	CTGCCACGTGAGGC CGCCCACGTGACCG GGGTCAGCTGATCC	**-588** **17** **49**
	cathepsin F	Unknown	*CTSF*	1.7 ± 0.5	2.1 ± 0.8	n.d.	AGCTCAGGTGATCT GGTTCAAGTGATTC ACCTCAGGTGATCC GCCCCACGTGCCTC	**-997** **-476** **-341** **-84**
	cathepsin K	Pycnodysostosis	*CTSK*	1.2 ± 0.2	1.5 ± 0.3	n.d.	AGCTCATGTGACTT	**-633**
	cathepsin O	Unknown	*CTSO*	1.6 ± 0.4	1.5 ± 0.5	n.d.	AGGCCAGGTGGCTC GAGGCACTTGAACC TGGTCAAGTGCCTG	**-489** **-309** **-193**
	alpha glucosidase	Pompe disease	*GAA*	1.6 ± 0.7	2.0 ± 0.8	n.d.	GCGTCACGTGACCC CGGTCACGTGACCC	**-54** **-9**
	beta glucosidase	Lewy body dementia, Gaucher	*GBA*	1.4 ± 0.4	1.6 ± 0.2	1.8 ± 0.1	GTGTCATGTGACGC GTGTCATGTGACGC TCATCACATGACCC TCATCACATGACCC	**-24** **-21** **-4** **1**
	N-acetylglucosamine-6-sulfatase	Mucopolysaccharidosis IIID	*GNS*	1.2 ± 0.2	1.4 ± 0.1	1.6 ± 0.1	ACCTCAGGTGATCC CCGTCACGTGACCG GGCTCACGTGATCG	**-905** **-29** **13**
	alpha-L-fucosidase	Fucosidosis	*FUCA1*	1.6 ± 0.5	1.6 ± 0.2	n.d.	GGCTCAAGCGATCC	**-424**
	hexosaminidase A	GM2 Gangliosidoses	*HEXA*	1.4 ± 0.2	1.6 ± 0.4	1.6 ± 0.1	GAGTCGGGTGAGCT TGGTCACGTGATTC CGCTCACCTGACCA GTCTCACGTGGCCA	**-101** **115** **150** **166**
	hexosaminidase B	GM2 Gangliosidoses	*HEXB*	1.4 ± 0.1	1.2 ± 0.0	n.d.	TCGTCATGTGACTT ACCTCAGGTGATCC CAGTCATCTGACTC	**-871** **-237** **4**
	hexosaminidase C	GM2 Gangliosidoses	*HEXDC*	1.1 ± 0.0	1.6 ± 0.5	n.d.	CGCCCACCTGCCCC	**-90**
	hyaluronoglucosaminidase 3	Unknown	*HYAL3*	1.7 ± 0.5	1.0 ± 0.1	n.d.	GCCCCACCTGATCG GCCCCACCTGATCG GGAGCAGGTGAGTA GGCTCAGCTGCCCG	**-891** **-285** **166** **189**
	alpha L-iduronidase	Mucopolysaccharidosis I	*IDUA*	1.4 ± 0.3	1.3 ± 0.2	1.4 ± 0.2	GCCTCAAGTGATCC CGGTCACATGGGGT	**-850** **1**
	legumain	Unknown	*LGMN*	1.4 ± 0.3	1.8 ± 0.3	n.d.	AAATCACCTGAGGC	**-869**
	alpha mannosidase	Alpha-Mannosidosis	*MAN2B1*	1.3 ± 0.4	1.9 ± 0.7	1.6 ± 0.1	GGTTCAAGTGATTC GGCCCAAGTGATTC	**-798** **-625**
	beta mannosidase	Beta-Mannosidosis	*MANBA*	2.4 ± 0.8	2.4 ± 0.5	5.1 ± 1.1	CGCTCAGCTGACCT	**-38**
	alpha-N-	Mucopolysaccharidosis	*NAGLU*	1.6 ± 0.5	1.3 ± 0.2	1.8 ± 0.6	GGCTCACATGGCCC CGGTCACGAGACGC	**-321** **179**

TABLE 3—*continued*

	acetylglucosaminidase	IIIB						
	sialidase 1	Sialidosis, Galactosialidosis	*NEU1*	2.9 ± 0.4	2.5 ± 0.3	n.d.	GGATCACCTGAGTC GGGTCACGCGCTCC TGATCACGTGGGAG GGGTCAGCTGACTC	**-535** **-91** **-18** **96**
	phospholipase B domain containing 2	Unknown	*P76/PLBD2*	1.4 ± 0.2	1.5 ± 0.3	n.d.	-	-
	mitochondrial carrier 1	Unknown	*PSAP*	1.3 ± 0.0	1.4 ± 0.2	n.d.	CCACCACCTGCCCC CCCCCACGTGCCCC GGATCAGCTGACGC	**-479** **-469** **60**
	serine carboxypeptidase 1	Unknown	*SCPEP1*	1.4 ± 0.2	1.5 ± 0.1	n.d.	CCGTCACGTGATGG	**-6**
	N-sulfoglucosamine sulfohydrolase	Mucopolysaccharidosis IIIA	*SGSH*	1.4 ± 0.3	1.0 ± 0.3	2.1 ± 0.4	GCGCCACCTGACCG CGCGCACGTGACCG	**-312** **-8**
	sphingomyelin phosphodiesterase 1	Niemann-Pick disease type A, B	*SMPD1*	1.4 ± 0.2	1.7 ± 0.2	1.9 ± 0.2	-	-
	tripeptidyl peptidase	Late-infantile neuronal ceroid lipofuscinosis	*TPP1*	2.0 ± 0.5	1.6 ± 0.2	n.d.	AGGTCAAATGATCG TATCCACCTGAGCC AGCTCATGTGATCC CCGTCACATGACAG	**-976** **-585** **18** **30**
Lysosomal membrane proteins	chromosome 1 open reading frame 85	Unknown	*C1orf85*	1.5 ± 0.4	1.5 ± 0.2	n.d.	GATTCAAGTGATTC GGATCAGCTGAACG GAGTCATGTGACCC CCGCCAGGTGAGGG	**-782** **-19** **-4** **160**
	sialomucin	Unknown	*CD164*	1.3 ± 0.6	1.3± 0.3	n.d.	GCCTCAGCTGCCCA AGGTCACGTGGGCC CTCTCACGTGACCC	**-528** **-275** **57**
	CD68 molecule	Unknown	*CD68*	1.8 ± 0.2	1.4 ± 0.1	n.d.	ACCTCAGCTGAGCT ACCTCAGCTGAGCT GGATCAACTGCCCT GGATCAACTGCCCT	**-718** **-717** **-84** **-83**
	MFS transporter, ceroid-lipofuscinosis neuronal protein 7	Late-infantile neuronal ceroid lipofuscinosis	*CLCN7*	1.2 ± 0.3	1.4 ± 0.4	n.d.	GGATCACTTGAGGT AGGTCACATGGTCG TCATCACGTGGCCC GCGTCACGTGGCCG GGGTCACGAGAACA	**-963** **-15** **8** **28** **49**
	ceroid-lipofuscinosis, neuronal protein 3	Juvenile neuronal ceroid lipofuscinosis/Batten Disease	*CLN3*	1.4 ± 0.4	1.4 ± 0.3	n.d.	GGATCACCTGAGCC GGCACAAGTGATCC GGCACAAGTGATCC TGAGCACGTGATGG CTGTCACGTGATCC	**-836** **-660** **-440** **-25** **6**
	ceroid-lipofuscinosis neuronal protein 5	Late-infantile neuronal ceroid lipofuscinosis	*CLN5*	2.5 ± 0.3	2.1 ± 0.4	n.d.	AGGTCGGGTGACGA	**-303**
	cystinosin	Cystinosis	*CTNS*	1.5 ± 0.4	1.6 ± 0.2	n.d.	AACTCACCTGGGGC	**-422**
	mucolipin 1	Mucolipidosis IV	*MCOLN1*	1.2 ± 0.4	1.5 ± 0.2	n.d.	GGCTCAAGCGATCC CGGTCACGTGAGGG GGGTCACGTGACCG AGATCAGCTGATGC GGCTCAGGTGAGGG	**-877** **-30** **-3** **19** **168**
	Niemann-Pick C1-like protein 1	Niemann-Pick disease type C	*NPC1*	1.4 ± 0.4	2.3 ± 0.4	n.d.	CTTTCAGGTGACTG	**-273**
	Niemann-Pick C1-like protein 2	Niemann-Pick disease type C	*NPC2*	1.3 ± 0.3	1.4 ± 0.1	n.d.	AGGTCGCCTGACTG	**6**
	solute carrier family 11, member 2	Unknown	*SLC11A2*	1.4 ± 0.2	1.5 ± 0.1	n.d.	GGCCCAAGTGATTC ATCTCAGGTGATTC ACCTCAGGTGGTCC GACTCAAGTGATCC ATCTCAGGTGATTC GACTCAAGTGATCC GTGTCAGGTGGTTG GTGTCAGGTGGTTG	**-845** **-823** **-699** **-677** **-548** **-402** **-194** **83**
	solute carrier family 36, member 1	Unknown	*SLC36A1*	1.0 ± 0.3	1.3 ± 0.2	n.d.	GGAGCACGTGACCT GGATCACGTGATGA	**-45** **-10**
	sortilin 1	Unknown	*SORT1*	1.3 ± 0.2	1.4 ± 0.2	n.d.	-	-
Lysosomal acidification	V-type H+-transporting ATPase subunit I	Unknown	*ATP6V0A1*	1.5 ± 0.3	1.6 ± 0.2	n.d.	-	-
	V-type H+-transporting ATPase 21kDa proteolipid subunit B	Unknown	*ATP6V0B*	1.1 ± 0.1	1.4 ± 0.1	n.d.	AAGTCAGCTGAGGG GGGTCACGTGGTAC GCATCACGTGGGCG GAGTTAGGTGACGC	**-597** **-30** **-12** **3**
	V-type H+-transporting ATPase subunit A	Unknown	*ATP6V1A*	1.3 ± 0.1	1.4 ± 0.1	n.d.	AGATCACGTGATTG ACGTCATGTGACTG CCAGCAGGTGAGCG	**-324** **-31** **91**

TABLE 3—*continued*

	V-type H+-transporting ATPase subunit B1	Unknown	*ATP6V1B1*	1.9 ± 0.5	1.4 ± 0.2	n.d.	CTCTCAGGTGACGG	**-159**
	V-type H+-transporting ATPase subunit C1	Unknown	*ATP6V1C1*	1.1 ± 0.0	1.6 ± 0.6	n.d.	CGGTCAGCTGACTG CTGGCACGTGACTT	**33** **52**
	V-type H+-transporting ATPase subunit G	Unknown	*ATP6V1G1*	1.4 ± 0.2	1.4 ± 0.1	n.d.	TCCTCACCTGAAGT CGGTCAGCTGATGC CGGTCACGTGACAA GTGTCAGCTGACCC	**-838** **-29** **-6** **58**
	V-type H+-transporting ATPase subunit H	Unknown	*ATP6V1H*	1.1 ± 0.1	1.3 ± 0.3	n.d.	GGTTCAAGTGATTT TGGTCAGCTGGTCT ACCTCAGGTGATCC CAGTCACGTGCCTC CGATCACGTGACCG CAGTCACGTGCCTC CGATCACGTGACCG AGGTCAGGCGACTC	**-870** **-759** **-735** **-266** **-252** **5** **19** **53**
Other lysosomal enzymes, activators and lysosome-associated units	GM2 ganglioside activator	Gangliosidosis	*GM2A*	1.7 ± 0.4	1.5 ± 0.6	2.1 ± 0.2	-	-
	N-acetylglucosamine-1-phosphate transferase, alpha and beta subunits	Mucolipidosis II and III	*GNPTAB*	1.2 ± 0.5	1.9 ± 0.1	n.d.	-	-
	insulin-like growth factor 2 receptor	Unknown	*IGF2R*	1.3 ± 0.3	1.5 ± 0.3	n.d.	CGCTCACGTGACCC GGGTCACCTGAACA GAGTCACGTGAGCG CTGTCACGTGACGC	**-152** **-111** **-94** **-48**
	palmitoyl-protein thioesterase 1	Infantile neuronal ceroid lipofuscinosis	*PPT1*	1.4 ± 0.2	1.1 ± 0.2	n.d.	-	-
	cation-dependent mannose-6-phosphate receptor	Unknown	*M6PR*	1.1 ± 0.2	1.3 ± 0.0	n.d.	CCGCCACCTGCCCC CAGGCGCGTGACCC TGGTCACATGCCGC	**-233** **-182** **44**
	Ras-related GTP binding C	Unknown	*RRAGC*	1.4 ± 0.3	1.0 ± 0.3	n.d.	GAGTCAGGTGATTC CCGGCACGTGACGG	**-232** **-219**
	sulfatase modifying factor 1	Mucosulphatidosis	*SUMF1*	1.6 ± 0.2	1.7 ± 0.3	n.d.	CAGCCACGTGACCA GGGTCACATGGCCC	**-3** **16**
	GABA(A) receptor-associated protein	Unknown	*GABARAP*	1.3 ± 0.3	1.3 ± 0.3	n.d.	CCGCCACGTGACGC	**-638**
	ATP-binding cassette, sub-family A (ABC1), member 9	Unknown	*ABCA9*	1.1 ± 0.4	1.6 ± 0.4	n.d.	TCACCACGTGAGCA	**-81**
	follicular lymphoma variant translocation 1	Unknown	*FVT1*	1.3 ± 0.2	1.4 ± 0.4	n.d.	-	-
Autophagy	sequestosome 1	Unknown	*SQSTM1*	2.4 ± 0.4	1.7 ± 0.1	n.d.	GAGTCACTTGGACC CGCCCAGGTGCGCC GCGCCAGGTGCGGG CGCCCAGGTGCGCC GCGCCAGGTGCGGG	**-634** **-559** **-550** **58** **67**
	vacuolar protein sorting 11 homolog	Unknown	*VPS11*	1.2 ± 0.2	1.4 ± 0.4	n.d.	GGCTCAAGTGATTC CGACCACGTGATTC AGCTCACGTGACAA	**-583** **-23** **1**

* n.d., no data available.
** Position is relative to the transcription start site.

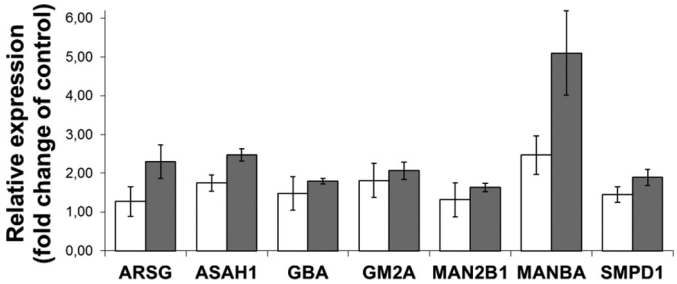

FIGURE 3. **Selected genes encoding lysosomal enzymes involved in degradation pathways of composites stored in the cells of patients with lysosomal storage disease for which transcriptomic profiling using DNA microarrays (*white columns*) and real-time qRT-PCR (*gray columns*), normalized relative to *GAPDH*, revealed increased expression with -fold change ≥1.3 value (24-h treatment with 100 μM genistein).** Data represent averaged values ± S.D. from $n \leq 3$.

HEXB, *HYAL3*, *IDUA*, *NAGLU*, and *SGSH*), being differentially expressed after genistein treatment, were significantly enriched in their transcript level. Actions of products of these genes at particular reactions in the GAG metabolic pathways are shown in Fig. 5. Remarkably, most time-dependent changes in GAG metabolism gene expression occurred by 24 h for both genistein doses (*i.e.* 60 and 100 μM), although a reduced number of specific transcripts with increased and decreased expression (from 12 to 7 and from 16 to 9, at 60 and 100 μM genistein, respectively) after that time was observed (Table 2 and Fig. 6, *A* and *B*). In addition, 50% of genes among those whose mRNAs were expressed at differential levels were reliably regulated after 48 h of genistein treatment when compared with the 24-h time period (for 100 μM, see Fig. 6*B*).

Real-time qRT-PCR Analysis of Expression of Genes Involved in Glycosaminoglycan Metabolism—In summary, 11 genes, six of which (*i.e. CHPF*, *EXT1*, *GLCE*, *HS2ST1*, *ST3GAL2*, and *XYLT1*) are involved in the GAG synthesis and five in glycosaminoglycan degradation (*i.e. GNS*, *HEXA*, *IDUA*, *NAGLU*, and *SGSH*), being significantly regulated after 24 h of genistein

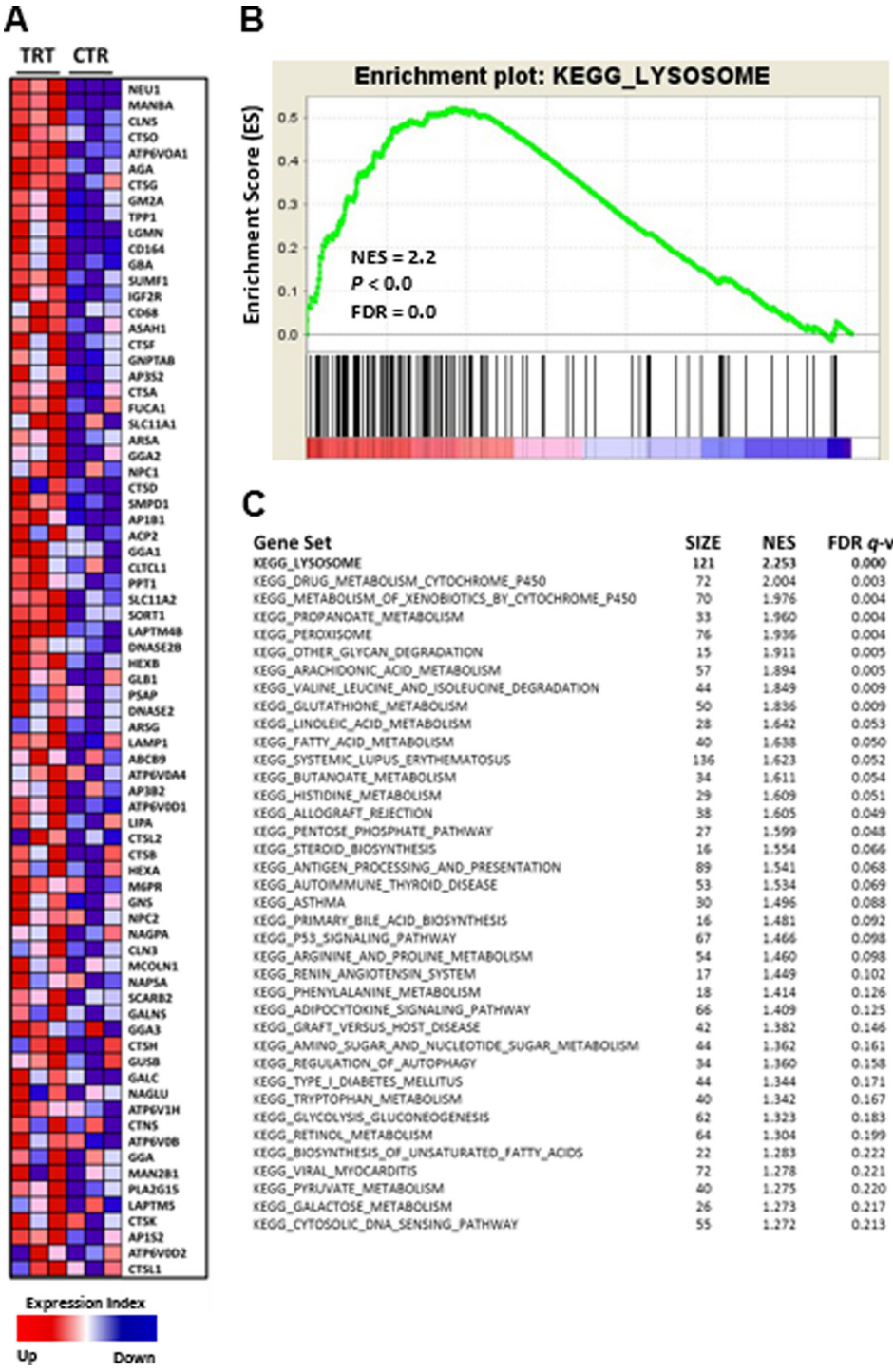

C

Gene Set	SIZE	NES	FDR *q*-val
KEGG_LYSOSOME	**121**	**2.253**	**0.000**
KEGG_DRUG_METABOLISM_CYTOCHROME_P450	72	2.004	0.003
KEGG_METABOLISM_OF_XENOBIOTICS_BY_CYTOCHROME_P450	70	1.976	0.004
KEGG_PROPANOATE_METABOLISM	33	1.960	0.004
KEGG_PEROXISOME	76	1.936	0.004
KEGG_OTHER_GLYCAN_DEGRADATION	15	1.911	0.005
KEGG_ARACHIDONIC_ACID_METABOLISM	57	1.894	0.005
KEGG_VALINE_LEUCINE_AND_ISOLEUCINE_DEGRADATION	44	1.849	0.009
KEGG_GLUTATHIONE_METABOLISM	50	1.836	0.009
KEGG_LINOLEIC_ACID_METABOLISM	28	1.642	0.053
KEGG_FATTY_ACID_METABOLISM	40	1.638	0.050
KEGG_SYSTEMIC_LUPUS_ERYTHEMATOSUS	136	1.623	0.052
KEGG_BUTANOATE_METABOLISM	34	1.611	0.054
KEGG_HISTIDINE_METABOLISM	29	1.609	0.051
KEGG_ALLOGRAFT_REJECTION	38	1.605	0.049
KEGG_PENTOSE_PHOSPHATE_PATHWAY	27	1.599	0.048
KEGG_STEROID_BIOSYNTHESIS	16	1.554	0.066
KEGG_ANTIGEN_PROCESSING_AND_PRESENTATION	89	1.541	0.068
KEGG_AUTOIMMUNE_THYROID_DISEASE	53	1.534	0.069
KEGG_ASTHMA	30	1.496	0.088
KEGG_PRIMARY_BILE_ACID_BIOSYNTHESIS	16	1.481	0.092
KEGG_P53_SIGNALING_PATHWAY	67	1.466	0.098
KEGG_ARGININE_AND_PROLINE_METABOLISM	54	1.460	0.098
KEGG_RENIN_ANGIOTENSIN_SYSTEM	17	1.449	0.102
KEGG_PHENYLALANINE_METABOLISM	18	1.414	0.126
KEGG_ADIPOCYTOKINE_SIGNALING_PATHWAY	66	1.409	0.125
KEGG_GRAFT_VERSUS_HOST_DISEASE	42	1.382	0.146
KEGG_AMINO_SUGAR_AND_NUCLEOTIDE_SUGAR_METABOLISM	44	1.362	0.161
KEGG_REGULATION_OF_AUTOPHAGY	34	1.360	0.158
KEGG_TYPE_I_DIABETES_MELLITUS	44	1.344	0.171
KEGG_TRYPTOPHAN_METABOLISM	40	1.342	0.167
KEGG_GLYCOLYSIS_GLUCONEOGENESIS	62	1.323	0.183
KEGG_RETINOL_METABOLISM	64	1.304	0.199
KEGG_BIOSYNTHESIS_OF_UNSATURATED_FATTY_ACIDS	22	1.283	0.222
KEGG_VIRAL_MYOCARDITIS	72	1.278	0.221
KEGG_PYRUVATE_METABOLISM	40	1.275	0.220
KEGG_GALACTOSE_METABOLISM	26	1.273	0.217
KEGG_CYTOSOLIC_DNA_SENSING_PATHWAY	55	1.272	0.213

FIGURE 4. *A*, GSEA-derived heat map of lysosome-associated genes in the leading edge showing the strongest up-regulation after genistein treatment (*TRT*) *versus* control (*CTR*) based on a signal/noise ratio (*SNR*) score. In *B*, the graph shows the enrichment plots generated by GSEA analysis of ranked gene expression data (*left*, up-regulated (*red*); *right*, down-regulated (*blue*)). The enrichment score is shown as a *green line*, and the *vertical black bars below* the plot indicate the positions of lysosome-associated genes, which are mostly grouped in the fraction of up-regulated genes (enrichment score = 0.52; $p < 0.001$). *C*, table of selective gene sets enriched among genes up-regulated by genistein in fibroblasts based on GSEA (*SIZE*, number of genes in each set; *NES*, normalized enrichment score; *FDR q-val*, *q* value of false discovery rate), with the lysosome gene set at the *top*.

treatment, were included in the real-time qRT-PCR verification using endogenous references *GAPDH* (Fig. 7*A*) and *TBP* (data not shown because qualitatively similar results were obtained as in the case of *GAPDH*). Measurements determined by the two transcript assessment systems showed a strong correlation ($R^2 = 0.77$ in *GAPDH*-controlled and 0.62 in *TBP*-controlled experiments for log-transformed ratios). The slope of the best fit line was 1.2 (for *GAPDH*) and 0.8 (for *TBP*), indicating that the ratios obtained by the two methods are similar in magnitude (Fig. 7*B*). Although a genistein-mediated decreased expression of some genes whose products are involved in GAG biosynthesis could be expected on the basis of previous reports

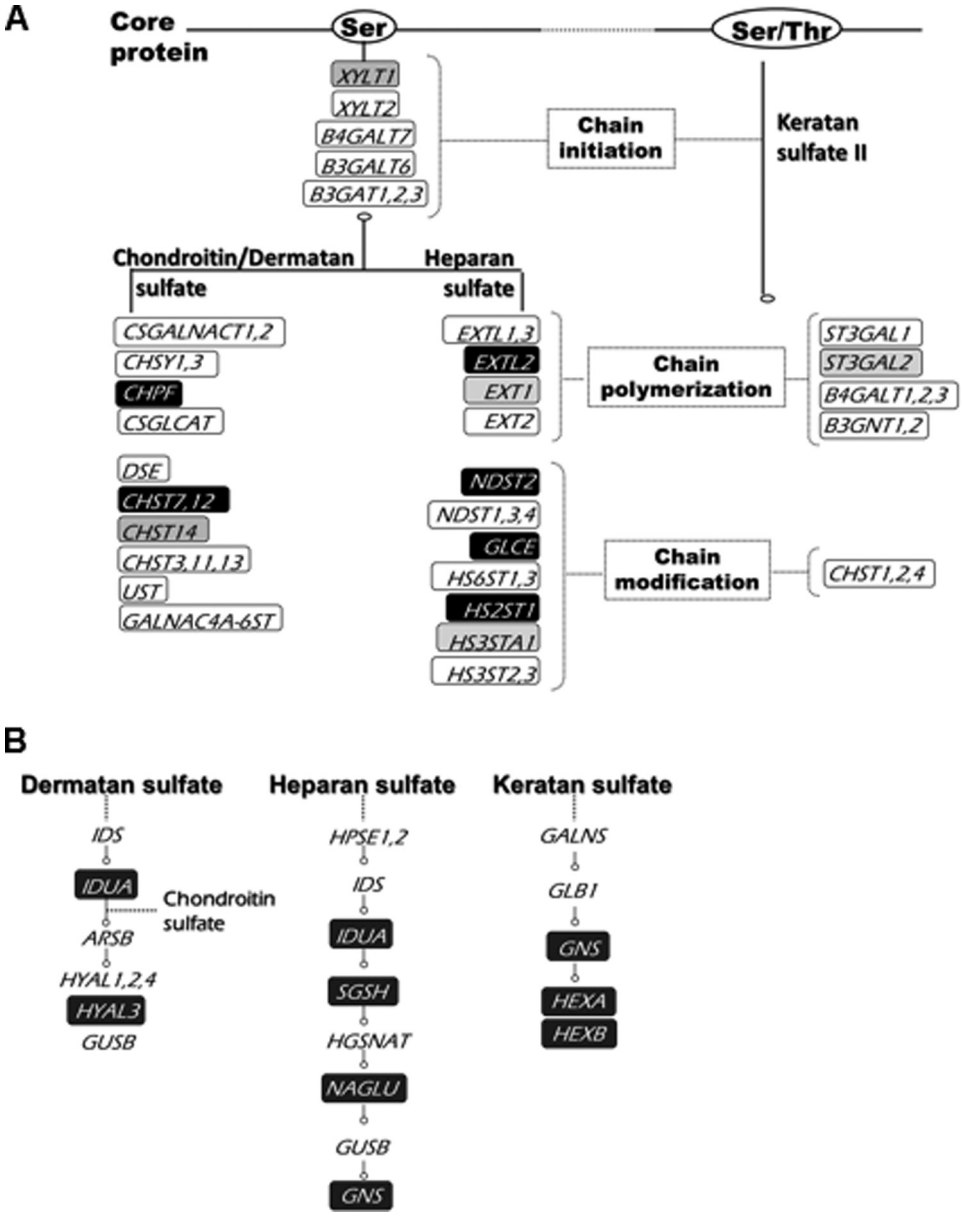

FIGURE 5. **A scheme for GAG biosynthesis (chondroitin/dermatan and heparan sulfate synthesis and keratan sulfate synthesis pathway) (*A*) and degradation (*B*).** Genes whose expression in both the microarray and real-time qRT-PCR analyses is stimulated in HDFa cells by genistein are *shaded* in *black*, and genes whose expression is inhibited by genistein are *shaded* in *gray*.

(20), the enhanced levels of mRNAs for glycosaminoglycan-degrading enzymes in the presence of genistein were surprising.

TFEB Expression Level Assessment and Its Subcellular Localization—The recently discovered CLEAR gene network activating lysosomal biogenesis commanded by the TFEB (21, 22) prompted us to investigate whether genistein treatment may affect TFEB expression in HDFa. Interestingly, we found that genistein induced a 2-fold increase of TFEB mRNA level compared with the non-treated counterpart by using the *GAPDH* (Fig. 8*A*) reference control gene. No microarray data regarding modulation of expression of *TFEB* gene were available due to the problem with low level analysis being related to elimination of the data for this particular sequence after background adjustment. To further confirm the latter results, we investigated the expression of endogenous TFEB after genistein treatment by using mouse embryonic fibroblasts isolated from a knock-in mouse where the reporter gene β-galactosidase was inserted in one allele of the *TFEB* gene locus. We found that genistein induced a concentration-dependent increase of the reporter protein and, therefore, TFEB expression (Fig. 8*B*). As shown by a representative blot in Fig. 8*C*, an increased protein level of TFEB was also detected in genistein-treated HDFa when compared with control samples. In addition, an increasing concentration of genistein determined the progressive translocation of TFEB from a diffused localization in the cytoplasm, where it mainly resides in untreated TFEB-FLAG HeLa, to the nucleus (Fig. 8*D*). Induction of TFEB nuclear translocation can also be induced by drugs that promote lysosomal stress (18); however, we were able to discard the hypothesis of a genistein-mediated induction of lysosomal membrane permeabilization by using the lysosomotropic fluorescent probe acridine orange in HeLa cells treated with genistein at different time

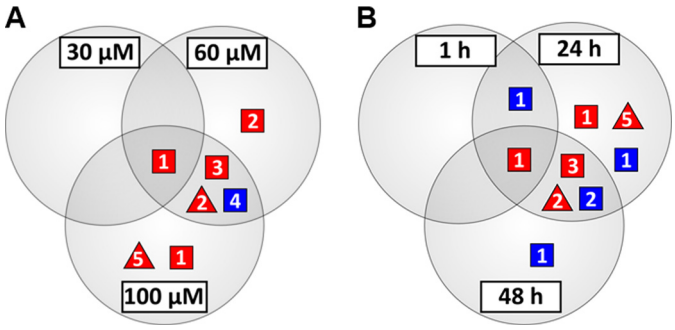

FIGURE 6. **Venn diagrams illustrating distribution of up-regulated (*black symbols*) and down-regulated (*white symbols*) GAG metabolism (*i.e.* synthesis (□) and degradation (△)) genes of HDFa cells after 24-h treatment with 30, 60, and 100 μM genistein (*A*) or 1-, 24-, and 48-h treatment with 100 μM genistein (*B*), made on the basis of microarray data, against non-treated samples, with respect to reference gene *GAPDH* of a constant expression.** The *digits inside* the *symbols* are numbers of transcripts identified as changed under studied conditions with corresponding overlap between the data sets.

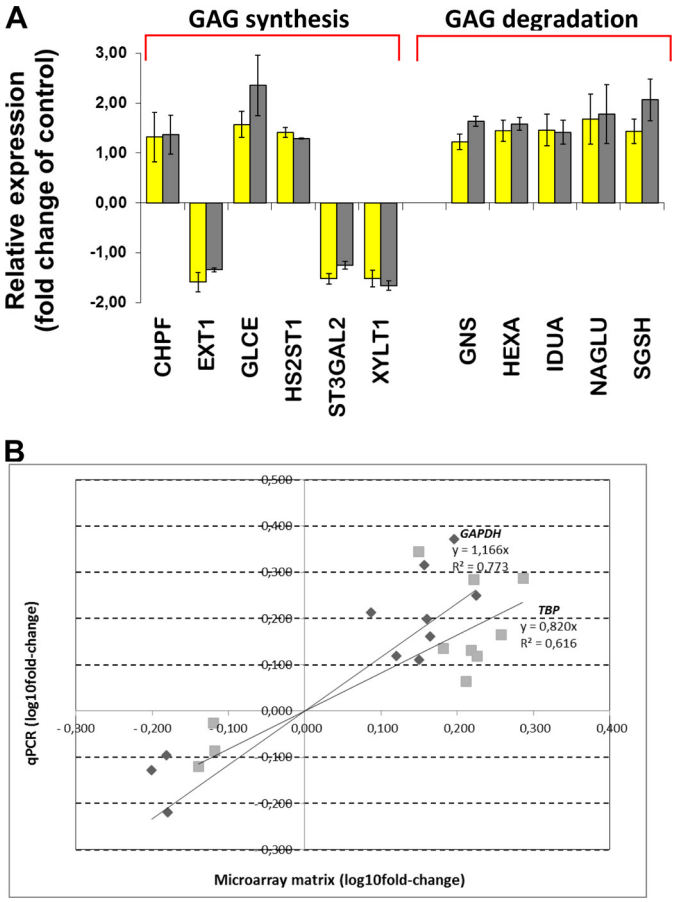

FIGURE 7. **Validation of microarray data of genes involved in glycosaminoglycan biosynthesis and degradation in HDFa cells by real-time qRT-PCR.** Based on the Illumina microarray analysis, alterations in the mRNA level of the selected genes after 24 h of 100 μM genistein treatment were considered as -fold change ≥1.3 with a p value of <0.01. The microarray (*white columns*) and real-time qRT-PCR (*gray columns*) data represent averaged values ± S.D. from $n = 5$ and $n \geq 3$, respectively, and denote significant differences for samples treated with genistein against non-treated samples, with respect to the reference gene *GAPDH* (*A*) of a constant expression. *B*, analysis of microarray and real-time qRT-PCR data correlation categorized by -fold change. The results of real-time qRT-PCR analysis for the selected genes were in direct agreement with the microarray data.

points and at a concentration that promotes maximal TFEB nuclear translocation (Fig. 9*A*). More interestingly, acridine orange-positive lysosomes were also increased in genistein-treated cells when compared with DMSO-treated control 24 h after treatment (Fig. 9*B*), suggesting an increase in the lysosomal number. To further confirm that the treatment with genistein increases the number of lysosomes, we investigated whether genistein was able to promote lysosomal biogenesis by staining with LysoTracker Red DN-99. Indeed, we found a significant increase in the number of lysosomes in genistein-treated HDFa as compared with non-treated control cells (Fig. 9*C*).

Effect of TFEB Knockdown on Genistein-mediated Induction of Lysosome-associated Genes—In order to investigate the contribution of TFEB activation to the genistein-mediated induction of lysosomal genes, we silenced the *TFEB* gene using specific siRNA oligonucleotides in HeLa cells treated with genistein (Fig. 10). In control genistein-treated cells, mRNA levels of endogenous TFEB as well as TFEB target genes (modulated by genistein and selected from Table 3) significantly increased, whereas in TFEB-depleted cells, the genistein response was considerably inhibited. These results suggest that the genistein-mediated transcriptional effect on lysosomal biogenesis is TFEB-dependent.

Identification of TFEB Direct Targets—To test whether lysosome-associated genes induced by genistein in this study are direct targets of TFEB, we performed a *de novo* CLEAR motif analysis. Pattern discovery analysis of the promoter regions of the 64 lysosome-associated genes resulted in the identification of CLEAR elements highly enriched in this promoter set (55 genes of 64; $p < 0.0001$) (Table 3). In 61% of the cases, two or more CLEAR sites were detected. We found that 153 promoters, corresponding to 55 genes, contained CLEAR-like sequences located within −1000 to +200 bp from the transcription start site. What is more, TFEB binding sites tend to be slightly more concentrated (64%) between positions −300 and +200 bp relative to the transcription start site. Additionally, distribution of this motif was determined around human gene transcription start sites of 467 genes that exhibited significant expression after genistein treatment (up- and down-regulated ≥2-fold). We focused our analysis on the regions spanning from −1000 to +200 bp from all annotated transcription start sites of human genes. Among 231 up-regulated and 236 down-regulated mRNAs in each case, 122 (53 and 52%, respectively) were found to have CLEAR elements, either as a single sequence or as multiple sites. Subsequently, these genes, probably representing TFEB targets, were used for gene ontology analysis (Table 4). The results showed a significant enrichment for categories related to intracellular, cytoskeletal, and organelle parts and regulation of cellular processes. It should be noted that some of the genes matched to more than one class.

DISCUSSION

Among many varied applications, genistein has been demonstrated previously to reduce the efficiency of glycosaminoglycan synthesis, leading to its reduced accumulation in MPS cells (7, 23, 24). It was assumed that genistein may impair GAG metabolism by affecting expression of certain genes; therefore, comprehensive transcriptomic studies, so far not reported in

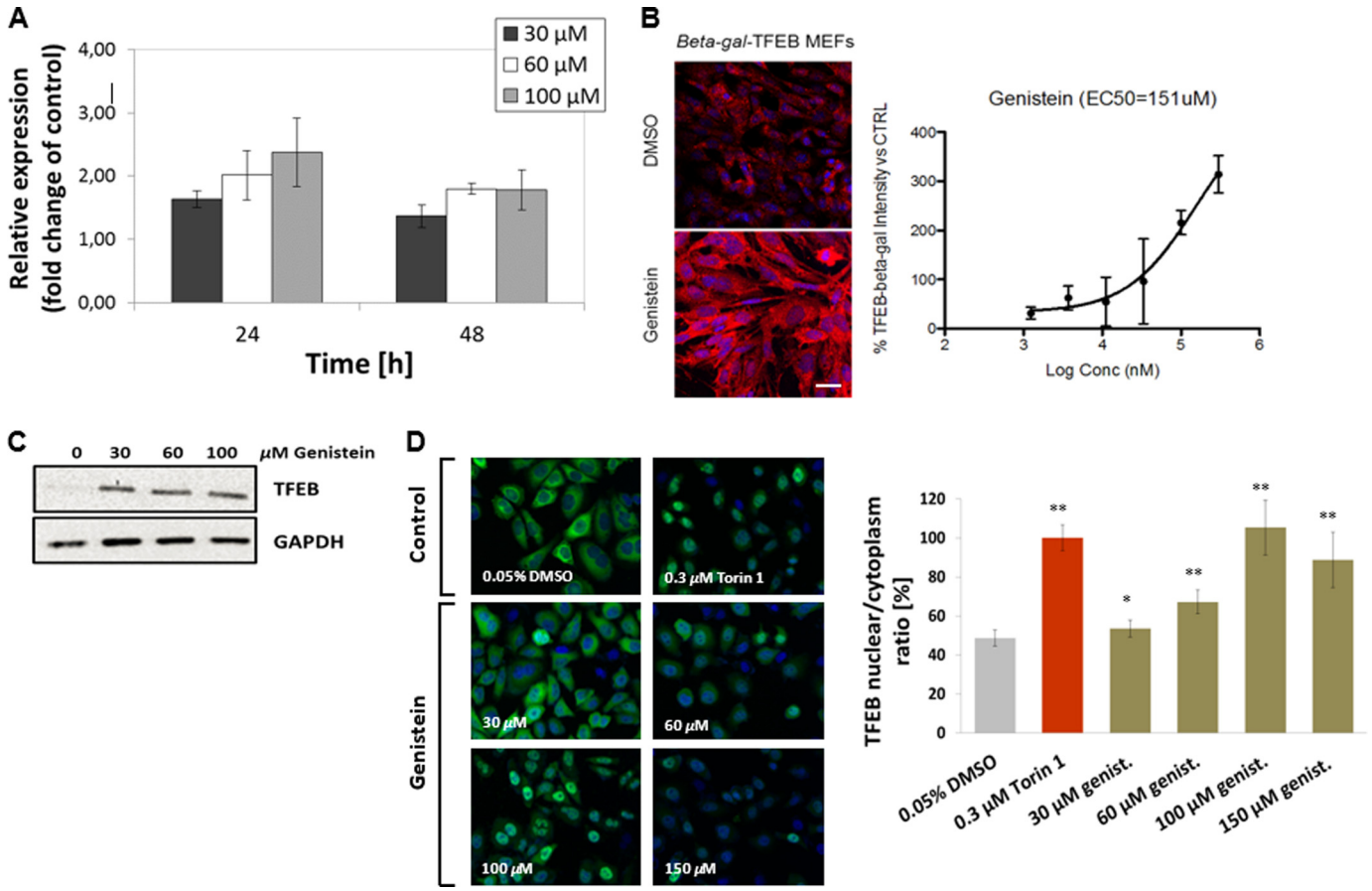

FIGURE 8. *A–C*, assessment of expression of endogenous TFEB in non-treated K2 and genistein-treated HDFa cells via real-time qRT-PCR (24- and 48-h treatment with 30, 60, and 100 μM, respectively, $p < 0.005$, as determined by analysis of variance with Tukey honestly significant difference post hoc) (*A*); a quantitative high content assay measuring β-galactosidase expression using mouse embryonic fibroblasts treated with genistein ranging from 30 to 300 μM (*B*); and Western blot analysis (48-h treatment with 30, 60, and 100 μM) (*C*). The real-time qRT-PCR data represent averaged values ± S.D. from $n = 3$ and denote significant differences for samples treated with genistein against untreated samples, with respect to reference gene *GAPDH* of a constant expression, whereas blots are representative of triplicate experiments. *D*, representative images of HeLa cells overexpressing TFEB cultured in medium with genistein for 24 h. Five fields containing 50–100 cells, each from six independent experiments, were analyzed for TFEB nuclear localization: nucleus stained with DAPI (*blue*); TFEB immunostained with FLAG (*green*). All values are means ± S.D. (Student's *t* test (unpaired); *, $p < 0.005$; **, $p < 0.00001$). *Scale bars*, 10 μm.

the literature, were strongly desired. Understanding the mechanism of genistein action in the light of cell transcriptome modulation may contribute to the implementation of this compound as a potential medication for mucopolysaccharidoses and other lysosomal storage diseases.

In this work, we addressed the gene profile signature after genistein treatment (Table 2). The analyses revealed, among hundreds of genes that displayed a greater than 2-fold increase or decrease in expression (for details see the NCBI Gene Expression Omnibus, GEO Series accession number GSE34074), a number of transcripts critically involved in the regulation of the cell cycle and associated with cellular metabolic oxidation-reduction processes, cell growth and division, and cytoskeletal, nucleosome and chromatin assembly (Fig. 2). Among them, 15 transcripts that displayed the most effective genistein-modulated expression (three up-regulated (*MT1X*, *MAOA* and *SLC40A1*) and 12 down-regulated (*KRT34*, *PCP4*, *RRM2*, *BCAT1*, *SERPINB13*, *BAIAP2L2*, *PLK4*, *HJURP*, *AURKB*, *CDCA8*, *GPR68*, and *RGS4*)) exhibited a 5–10-fold change in mRNA level after 24 h of treatment by genistein at 100 μM. Moreover, the altered expression of these genes occurred as early as after 24 h of treatment with genistein only at 30 and 60 μM and were significantly greater with longer treatment. We found that among the mRNA species with the most highly modulated expression, up-regulated *MT1X* and down-regulated *KRT34* are transcripts related to complications associated with mucopolysaccharidoses and other lysosomal storage diseases. Apart from *MT1X*, whose protein products can protect the cells from oxidative stress that is crucial for development of various lysosomal storage disease symptoms, being significantly altered (9-fold change) in fibroblasts treated for 24 h with 100 μM genistein, three other MT isoforms (*i.e. MT1A*, *MT1E*, and *MT1F* mRNAs) were also enriched by 2-fold and more. Considering the complex pathomechanism of mucopolysaccharidosis and a large spectrum of genistein activities, one may assume that this isoflavone can be beneficial in therapy for this disease due to not only its primary action as indirect GAG synthesis inhibitor and degradation enhancer but also its secondary, MPS-nonspecific, effects. As known from the literature, these include attenuation of oxidative stress in the brain (25, 26). Our results for the *KRT34* mRNA decrease (10-fold change) in fibroblasts treated for 24 h with 100 μM genistein also agree with our previous observations and those of several others who have studied hair morphology in MPS-affected patients on genis-

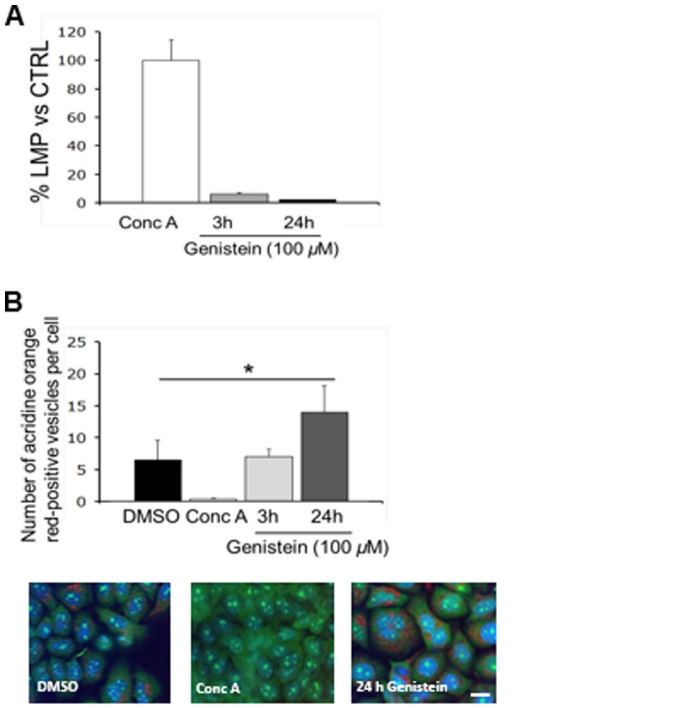

FIGURE 9. *A*, lysosomal membrane permeabilization detection in cell culture. HeLa cells were cultured for 3 and 24 h with 100 μM genistein and stained for 15 min with 5 μg/ml acridine orange. As a positive control of lysosomal membrane permeabilization, the cells were treated with the vesicular-proton pump inhibitor concanamycin A. *B*, quantitative analysis of the number of red puncta (acridine orange red spots) in cells treated with genistein; *, $p < 0.004$. Data represent averaged values ± S.D. *C*, genistein-mediated stimulation of lysosome amount and translocation (*arrows*) in fibroblasts. Shown are representative microscopy images of untreated and genistein-treated cells stained with LysoTracker (*red*). Nuclei were stained with DAPI (*blue*). *Scale bars*, 10 μm.

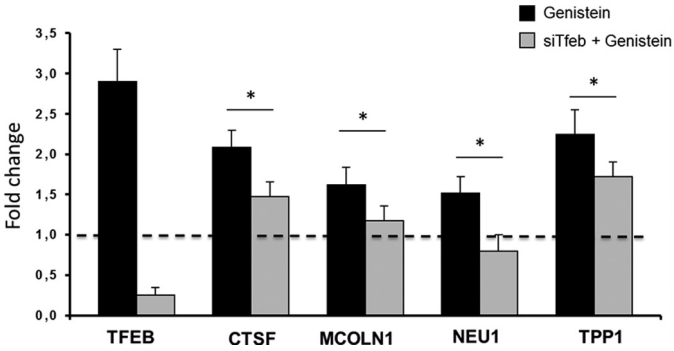

FIGURE 10. **Quantification of the effect of *TFEB* knockdown on selected lysosome-associated gene activity up-regulated by genistein in HeLa cells.** Levels of mRNAs were analyzed by quantitative real-time PCR with *HPRT* used as a reference, and values are means ± S.D. of three independent experiments. *, $p < 0.05$.

TABLE 4
Gene ontology (GO) analysis of CLEAR genes whose expression changed ≥2-fold in response to genistein

GO Term	Description	Gene count	*p*-value	FDR *q*-value	Fold enrichment
	Cellular compartment				
GO:0044424	*intracellular part*	185	3,21E-04	1,44E-02	1.14
GO:0043226	*organelle*	156	1,42E-06	1,31E-04	1.29
GO:0044430	*cytoskeletal part*	43	1,65E-08	3,82E-06	2.51
GO:0044427	*chromosomal part*	19	1,44E-04	6,93E-03	2.60
GO:0032993	*protein-DNA complex*	9	2,13E-04	9,88E-03	4.42
GO:0045171	*intercellular bridge*	5	6,59E-05	3,67E-03	11.53
	Biological process				
GO:0009987	*cellular process*	189	4,17E-05	8,72E-03	1.16
GO:0071840	*cellular component organization or biogenesis*	78	1,77E-05	4,40E-03	1.55
GO:0022402	*cell cycle process*	52	4,69E-19	5,70E-15	4.19
GO:0009056	*catabolic process*	41	1,57E-04	2,50E-02	1.79
GO:0051128	*regulation of cellular component organization*	39	2,37E-05	5,32E-03	2.00
GO:0033554	*cellular response to stress*	32	2,05E-05	4,89E-03	2.21
GO:0010941	*regulation of cell death*	31	6,75E-04	7,96E-02	1.85
GO:0010564	*regulation of cell cycle process*	28	3,52E-12	1,43E-08	4.92
	Molecular function				
GO:0003824	*catalytic activity*	94	2,28E-04	6,09E-02	1.37
GO:0043168	*anion binding*	54	1,21E-04	5,40E-02	1.64
GO:0032553	*ribonucleotide binding*	40	7,31E-04	1,39E-01	1.68
GO:0008092	*cytoskeletal protein binding*	21	4,96E-04	1,04E-01	2.24
GO:0008514	*organic anion transmembrane transport*	8	3,58E-04	7,97E-02	4.61

tein (27–29). There are also two other genes, *HMOX1* and *MAOA*, whose expression is remarkably and significantly increased (4-fold change) in a genistein-dependent fashion. For *HMOX1*, it is well known that induction of its transcription reduces the damage caused by oxidative stress or inflammation (30, 31), whereas in the case of the monoamine oxidase A, its expression levels may be related to behavioral aggression and mental problems, which are also among the symptoms of mucopolysaccharidosis, particularly MPS II and III (32, 33). Obviously, the concept of a gene that directly relates to the disease effect is rather simplistic; therefore, a full pathway from the gene to complex behavior must still be studied, also when considering the effects of genistein on patient health improvement.

Both microarray and real-time qRT-PCR analyses indicated that genistein influences the expression of several genes involved in glycosaminoglycan metabolism (Fig. 7). Although the gene expression changes observed here are rather subtle, they appear to be relevant in cellular GAG level normalization. Our previous work documented, in fact, that alterations in transcription due to siRNA-mediated silencing of genes coding for enzymes involved in GAG synthesis lead to a decrease in the levels of the gene products directly contributing to the metabolism of glycosaminoglycans and impairment of GAG synthesis in transfected fibroblasts (34, 35). At this time, we report that among genes coding for enzymes involved in the glycosaminoglycan biosynthesis pathway and required for production of chondroitin/dermatan sulfate, heparan sulfate, and keratan sulfate, expressions of *EXT1*, *ST3GAL2*, and *XYLT1* were significantly impaired in the presence of genistein. It is worth noting that *EXT1* and *XYLT1* code for enzymes acting at the very early stages of production of heparan and chondroitin/dermatan sulfates, whereas the enzyme encoded by *ST3GAL2* catalyzes the initial phase of the keratan sulfate II synthesis pathway (Fig. 5*A*). Because the final efficiency of a biochemical reaction is

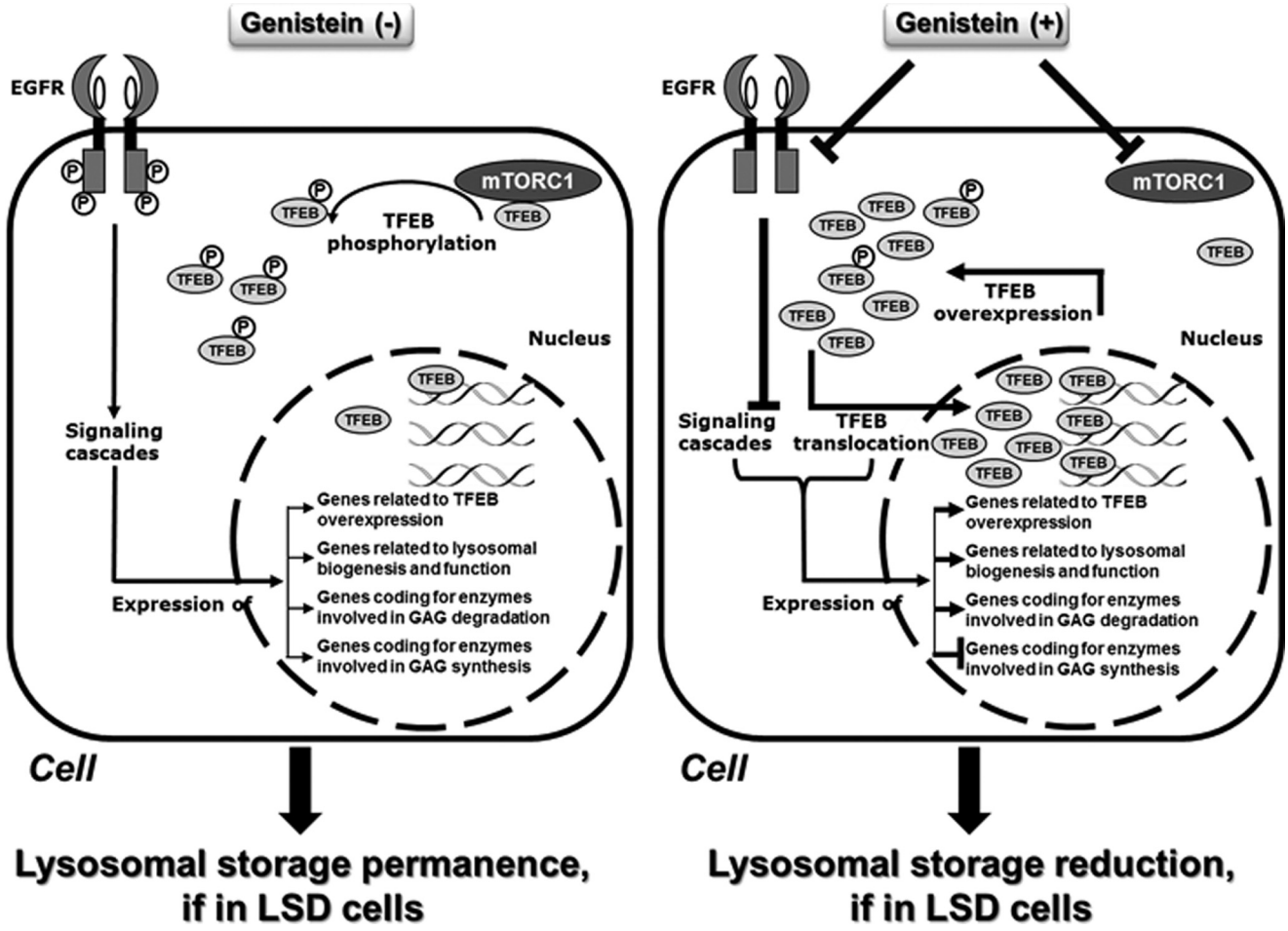

FIGURE 11. **Schematic representation of the putative mechanism of genistein regulating the lysosomal metabolism-related genes and *TFEB*.**

limited by the efficiency of its slowest step, it is likely that enhanced expression of *CHPF*, *GLCE*, and *HS2ST1* cannot reverse the effects of significantly decreased levels of mRNAs of *EXT1*, *ST3GAL2*, and *XYLT1* and thus the resulting low levels of corresponding enzymes and low efficiency of early steps of heparan sulfate and chondroitin/dermatan sulfate synthesis. Therefore, the final effect of genistein action is a decreased efficiency of production of chondroitin/dermatan, heparan, and keratan sulfates. This conclusion is corroborated by the results of earlier biochemical analyses (7, 11, 36). The altered expression signatures point to inhibition of signaling pathways as important targets for genistein, a candidate for mucopolysaccharidosis-inhibiting agent.

Interestingly, expression of the *AGA*, *ARSA*, *ARSG*, *ASAH1*, *FUCA1*, *GAA*, *GBA*, *GNS*, *HEXA*, *HEXB*, *HEXDC*, *HYAL3*, *IDUA*, *MAN2B1*, *MANBA*, *NAGLU*, *NEU1*, *SGSH*, *SMPD1*, *TPP1*, and *PPT1* genes, encoding hydrolases, of which 12 were confirmed by real-time qRT-PCR, was increased in the presence of genistein (Figs. 3 and 7). Some of these enzymes are involved in glycosaminoglycan degradation, and their dysfunctions cause different types of MPSs. Therefore, one might suppose that enhanced synthesis of products of those genes in the presence of genistein could result in an increased residual activity of the particular deficient enzyme. If this is true, patients suffering from MPS, who are treated with genistein, might benefit not only from less efficient accumulation of certain GAGs but also from its more effective degradation. Therefore, except for molecular basics for inhibition of gene expressions whose products are key elements in glycosaminoglycan biosynthesis, in this work, we also asked what is the mechanism for the genes' activation of lysosomal hydrolases by genistein. Interestingly, the analysis of "cellular compartment" as well as "biological processes" terms showed that enrichments for categories linked to the lysosome were among the significant ones (Fig. 2). We found 64 up-regulated genes encoding lysosomal proteins grouped into different classes (Table 3). These results are in substantial correlation with data previously reported by us (21, 22), where we discovered a transcription factor EB TFEB-mediated system (CLEAR) regulating the expression, import, and activity of lysosomal enzymes that control the degradation of proteins, glycosaminoglycans, sphingolipids, and glycogen (18, 21, 37–40). The majority of TFEB direct targets with a known role in lysosomal function already reported by us (37), were among those 64 lysosome-associated genes induced by genistein. Interestingly, of the 64 up-regulated genes, 55 (86%) were found to have CLEAR sequences in their promoters (Table 3). Furthermore, by monitoring particular mRNA levels in human and mouse fibroblasts with the use of real-time qRT- PCR, high content imaging, and Western blot, respectively (Fig. 8, *A*–*C*), we found that genistein also stimulates expression of the *TFEB*, demonstrated previously to act as a master positive regulator of lysosomal biogenesis (21, 37, 39). The necessary TFEB shuttling

from cytoplasm to the nucleus was also induced by genistein (Fig. 8*D*). In addition to genistein-mediated induction of TFEB target genes, we observed an increase in lysosomal biogenesis by measuring LAMP1 levels (Fig. 9*C*). Therefore, we conclude that enhancement of TFEB expression by genistein may cause stimulation of production of lysosomal hydrolases. Indeed, our results are consistent with those reported in the literature also describing that *TFEB* gene overexpression results in increased expression of genes encoding lysosomal enzymes, and under abnormal lysosomal storage conditions, TFEB translocates from the cytoplasm to the nucleus, resulting in the activation of genes with lysosomal function (18, 37).

In addition, we analyzed the effect of *TFEB* knockdown on lysosome-associated gene activity in cells treated with genistein. We observed a *TFEB* siRNA-mediated decrease in transcript levels of *CTSF*, *MCOLN1*, *NEU1*, and *TPP1* (Fig. 10). These results reveal a clear correlation between the activity of *TFEB* and genes whose expression was modulated by genistein. These data are in agreement with our bioinformatics studies, where we performed a CLEAR motif analysis of 64 up-regulated lysosome-associated genes induced by genistein. *CTSF*, *MCOLN1*, *NEU1*, and *TPP1* were among the 55 genes with CLEAR sequences in their promoters (Table 3).

Also, we combined our microarray data and genomic analysis to obtain a more comprehensive map of the TFEB targetome. CLEAR motif analysis of all genes whose expression was significantly altered (up- and down-regulated $\geq$2-fold) in response to genistein treatment (included in Table 2) revealed that more than half of them (52%) are controlled by the CLEAR network and belong to TFEB-mediated regulation. These TFEB target genes, when studied by gene ontology, were grouped in several categories (Table 4). The analysis of "cellular compartment," "biological process," and "molecular function" terms showed that enrichments for classes linked to intracellular parts, organelles, cellular process, and component organization or biogenesis were the most significant among TFEB targets.

Genistein has been demonstrated previously to inhibit synthesis of GAGs, possibly due to impairment of the kinase activity of epidermal growth factor receptor. The resultant halting of autophosphorylation of EGF receptor may cause a decrease in the efficiency of signal transduction and low level expression of genes coding for enzymes involved in glycosaminoglycan production. It was proposed that this mechanism is responsible for the already reported genistein-mediated decrease in storage of GAGs in cells derived from patients suffering from different types of mucopolysaccharidoses (11). However, our analyses of transcriptomes of human fibroblasts treated with genistein showed that this isoflavone not only inhibits the expression of genes coding for enzymes necessary for GAG synthesis but also stimulates the expression of genes coding for various lysosomal hydrolases. EGF is a ligand, which binds to a specific receptor (EGF receptor) and triggers a signal transduction pathway, resulting in activation of expression of certain genes. TFEB adjacent to master growth regulator mTORC1 (mammalian target of rapamycin complex 1) remains in a phosphorylated inactive form in the cytoplasm in the cell, whereas inhibition of mTORC1 by genistein, reported previously in the literature (41), may activate TFEB by promoting its nuclear translocation. Therefore, the following hypothesis emerges (Fig. 11). On the one hand, in the cells exposed to genistein, the EGF receptor phosphorylation is blocked by this isoflavone, so the impaired signal transduction pathway and modulation lead to reduced expression of several genes, including genes encoding enzymes of the GAG synthesis pathway, which in turn leads to reduced synthesis of this substrate in the cells. On the other hand, genistein-mediated mTORC1 inhibition of the TFEB phosphorylation appears to cause a translocation of the transcription factor EB from the cytoplasm to the nucleus, resulting in stimulation of certain lysosome-related gene expression and enhancement of degradation of lysosomal aggregates. Because this may be a potentially important mechanism of genistein-mediated reduction of storage of GAGs and other compounds accumulated in the cells of patients suffering from lysosomal storage diseases, TFEB may be a potential therapeutic target to enhance cellular clearance not only in MPS but generally in various lysosomal storage diseases. Furthermore, because TFEB plays an essential role in cell regulation, many possible side effects should be taken into consideration when thinking about genistein as a therapeutic drug.

As shown in many different studies, genistein may act through multiple pathways. Our results indicate indeed that genistein has an effect on regulating the expression of genes involved in metabolism of cell deposits in patients suffering from lysosomal storage disease, either by decreased expression of genes involved in the synthesis of the substrate or through increased expression of genes involved in the synthesis of lysosomal enzymes degrading specific substrates. Both approaches are relevant to substrate reduction therapy, due to the fact that the end result is a lower level of the substrate in the cells of lysosomal storage disease patients.

In conclusion, our current findings allowed us to learn about a putative genistein targetome responsible for impairment of production and enhancement of degradation of glycosaminoglycans. At the same time, this is the first study demonstrating directly that genistein alters the expression of genes involved in lysosomal metabolism.

Acknowledgment—We thank Dr. Katarzyna Potrykus for critical reading of the manuscript.

REFERENCES

1. Winchester, B., Vellodi, A., and Young, E. (2000) The molecular basis of lysosomal storage diseases and their treatment. *Biochem. Soc. Trans.* **28,** 150–154
2. Neufeld, E., Muenzer, J. (2001) in *Metabolic and Molecular Bases of Inherited Disease*, 8th Ed. (Scriver, C. R., Beaudet, A. L., Sly, W. S., and Valle, D., eds) pp. 3421–3452, McGraw-Hill, New York
3. Rohrbach, M., and Clarke, J. T. (2007) Treatment of lysosomal storage disorders: progress with enzyme replacement therapy. *Drugs* **67,** 2697–2716
4. Ponder, K. P., and Haskins, M. E. (2007) Gene therapy for mucopolysaccharidosis. *Expert Opin. Biol. Ther.* **7,** 1333–1345
5. Jakóbkiewicz-Banecka, J., Piotrowska, E., Gabig-Cimińska, M., Borysiewicz, E., Słomińska-Wojewódzka, M., Narajczyk, M., Węgrzyn, A., and Węgrzyn, G. (2011) Substrate reduction therapies for mucopolysaccharidoses. *Curr. Pharm. Biotechnol.* **12,** 1860–1865
6. Platt, F. M., and Jeyakumar, M. (2008) Substrate reduction therapy. *Acta Paediatr. Suppl.* **97,** 88–93
7. Piotrowska, E., Jakóbkiewicz-Banecka, J., Barańska, S., Tylki-Szymańska, A., Czartoryska, B., Wegrzyn, A., and Wegrzyn, G. (2006) Genistein-me-

diated inhibition of glycosaminoglycan synthesis as a basis for gene expression-targeted isoflavone therapy for mucopolysaccharidoses. *Eur. J. Hum. Genet.* **14,** 846–852
8. Malinowska, M., Wilkinson, F. L., Bennett, W., Langford-Smith, K. J., O'Leary, H. A., Jakobkiewicz-Banecka, J., Wynn, R., Wraith, J. E., Wegrzyn, G., and Bigger, B. W. (2009) Genistein reduces lysosomal storage in peripheral tissues of mucopolysaccharide IIIB mice. *Mol. Genet. Metab.* **98,** 235–242
9. Friso, A., Tomanin, R., Salvalaio, M., and Scarpa, M. (2010) Genistein reduces glycosaminoglycan levels in a mouse model of mucopolysaccharidosis type II. *Br J. Pharmacol.* **159,** 1082–1091
10. Malinowska, M., Wilkinson, F. L., Langford-Smith, K. J., Langford-Smith, A., Brown, J. R., Crawford, B. E., Vanier, M. T., Grynkiewicz, G., Wynn, R. F., Wraith, J. E., Wegrzyn, G., and Bigger, B. W. (2010) Genistein improves neuropathology and corrects behaviour in a mouse model of neurodegenerative metabolic disease. *PLoS One* **5,** e14192
11. Jakóbkiewicz-Banecka, J., Piotrowska, E., Narajczyk, M., Barańska, S., and Wegrzyn, G. (2009) Genistein-mediated inhibition of glycosaminoglycan synthesis, which corrects storage in cells of patients suffering from mucopolysaccharidoses, acts by influencing an epidermal growth factor-dependent pathway. *J. Biomed. Sci.* **16,** 26
12. Saeed, A. I., Bhagabati, N. K., Braisted, J. C., Liang, W., Sharov, V., Howe, E. A., Li, J., Thiagarajan, M., White, J. A., and Quackenbush, J. (2006) TM4 microarray software suite. *Methods Enzymol.* **411,** 134–193
13. Eden, E., Navon, R., Steinfeld, I., Lipson, D., and Yakhini, Z. (2009) GOrilla: a tool for discovery and visualization of enriched GO terms in ranked gene lists. *BMC Bioinformatics* **10,** 48
14. Subramanian, A., Tamayo, P., Mootha, V. K., Mukherjee, S., Ebert, B. L., Gillette, M. A., Paulovich, A., Pomeroy, S. L., Golub, T. R., Lander, E. S., and Mesirov, J. P. (2005) Gene set enrichment analysis: a knowledge-based approach for interpreting genome-wide expression profiles. *Proc. Natl. Acad. Sci. U.S.A.* **102,** 15545–15550
15. Kanehisa, M., Goto, S., Hattori, M., Aoki-Kinoshita, K. F., Itoh, M., Kawashima, S., Katayama, T., Araki, M., and Hirakawa, M. (2006) From genomics to chemical genomics: new developments in KEGG. *Nucleic Acids Res.* **34,** D354–357
16. Pfaffl, M. W., Tichopad, A., Prgomet, C., and Neuvians, T. P. (2004) Determination of stable housekeeping genes, differentially regulated target genes and sample integrity: BestKeeper: Excel-based tool using pair-wise correlations. *Biotechnol. Lett.* **26,** 509–515
17. Harlow, E., and Lane, D. (2006) Lysing tissue-culture cells for immunoprecipitation. *CSH Protoc.* 10.1101/pdb.prot4531
18. Settembre, C., Zoncu, R., Medina, D. L., Vetrini, F., Erdin, S., Erdin, S., Huynh, T., Ferron, M., Karsenty, G., Vellard, M. C., Facchinetti, V., Sabatini, D. M., and Ballabio, A. (2012) A lysosome-to-nucleus signalling mechanism senses and regulates the lysosome via mTOR and TFEB. *EMBO J.* **31,** 1095–1108
19. Antunes, F., Cadenas, E., and Brunk, U. T. (2001) Apoptosis induced by exposure to a low steady-state concentration of H_2O_2 is a consequence of lysosomal rupture. *Biochem. J.* **356,** 549–555
20. Węgrzyn, A. (2012) Gene expression-targeted isoflavone therapy. *IUBMB Life* **64,** 307–315
21. Sardiello, M., Palmieri, M., di Ronza, A., Medina, D. L., Valenza, M., Gennarino, V. A., Di Malta, C., Donaudy, F., Embrione, V., Polishchuk, R. S., Banfi, S., Parenti, G., Cattaneo, E., and Ballabio, A. (2009) A gene network regulating lysosomal biogenesis and function. *Science* **325,** 473–477
22. Settembre, C., De Cegli, R., Mansueto, G., Saha, P. K., Vetrini, F., Visvikis, O., Huynh, T., Carissimo, A., Palmer, D., Klisch, T. J., Wollenberg, A. C., Di Bernardo, D., Chan, L., Irazoqui, J. E., and Ballabio, A. (2013) TFEB controls cellular lipid metabolism through a starvation-induced autoregulatory loop. *Nat. Cell Biol.* **15,** 647–658
23. Wegrzyn, G., Jakóbkiewicz-Banecka, J., Gabig-Cimińska, M., Piotrowska, E., Narajczyk, M., Kloska, A., Malinowska, M., Dziedzic, D., Gołębiewska, I., Moskot, M., and Wegrzyn, A. (2010) Genistein: a natural isoflavone with a potential for treatment of genetic diseases. *Biochem. Soc. Trans.* **38,** 695–701
24. Banecka-Majkutewicz, Z., Jakobkiewicz-Banecka, J., Gabig-Ciminska, M., Wegrzyn, A., and Wegrzyn, G. (2012) Putative biological mechanisms of efficiency of substrate reduction therapies for mucopolysaccharidoses. *Arch. Immunol. Ther. Exp.* (*Warsz.*) **60,** 461–468
25. Chung, M. J., Kang, A. Y., Lee, K. M., Oh, E., Jun, H. J., Kim, S. Y., Auh, J. H., Moon, T. W., Lee, S. J., and Park, K. H. (2006) Water-soluble genistin glycoside isoflavones up-regulate antioxidant metallothionein expression and scavenge free radicals. *J. Agric. Food Chem.* **54,** 3819–3826
26. Liang, H. W., Qiu, S. F., Shen, J., Sun, L. N., Wang, J. Y., Bruce, I. C., and Xia, Q. (2008) Genistein attenuates oxidative stress and neuronal damage following transient global cerebral ischemia in rat hippocampus. *Neurosci. Lett.* **438,** 116–120
27. Delgadillo, V., O'Callaghan Mdel, M., Artuch, R., Montero, R., and Pineda, M. (2011) Genistein supplementation in patients affected by Sanfilippo disease. *J. Inherit. Metab. Dis.* **34,** 1039–1044
28. Narajczyk, M., Tylki-Szymańska, A., and Węgrzyn, G. (2012) Changes in hair morphology as a biomarker in gene expression-targeted isoflavone therapy for Sanfilippo disease. *Gene* **504,** 292–295
29. Piotrowska, E., Jakóbkiewicz-Banecka, J., Tylki-Szymanska, A., Liberek, A., Maryniak, A., Malinowska, M., Czartoryska, B., Puk, E., Kloska, A., Liberek, T., Baranska, S., Wegrzyn, A., and Wegrzyn, G. (2008) Genistein-rich soy isoflavone extract in substrate reduction therapy for Sanfillipo syndrome: an open-label, pilot study in 10 pediatric patients. *Curr. Ther. Res. Clin. Exp.* **69,** 166–179
30. Poss, K. D., and Tonegawa, S. (1997) Reduced stress defense in heme oxygenase 1-deficient cells. *Proc. Natl. Acad. Sci. U.S.A.* **94,** 10925–10930
31. Weis, S., Jesinghaus, M., Kovacs, P., Schleinitz, D., Schober, R., Ruffert, C., Herms, M., Wittenburg, H., Stumvoll, M., Blüher, M., Grützmann, R., Schulz, H. U., Keim, V., Mössner, J., Bugert, P., Witt, H., Drenth, J. P., Krohn, K., and Rosendahl, J. (2012) Genetic analyses of heme oxygenase 1 (HMOX1) in different forms of pancreatitis. *PLoS One* **7,** e37981
32. McDermott, R., Tingley, D., Cowden, J., Frazzetto, G., and Johnson, D. D. (2009) Monoamine oxidase A gene (MAOA) predicts behavioral aggression following provocation. *Proc. Natl. Acad. Sci. U.S.A.* **106,** 2118–2123
33. Węgrzyn, G., Jakóbkiewicz-Banecka, J., Narajczyk, M., Wiśniewski, A., Piotrowska, E., Gabig-Cimińska, M., Kloska, A., Słomińska-Wojewódzka, M., Korzon-Burakowska, A., and Węgrzyn, A. (2010) Why are behaviors of children suffering from various neuronopathic types of mucopolysaccharidoses different? *Med. Hypotheses* **75,** 605–609
34. Dziedzic, D., Wegrzyn, G., and Jakóbkiewicz-Banecka, J. (2010) Impairment of glycosaminoglycan synthesis in mucopolysaccharidosis type IIIA cells by using siRNA: a potential therapeutic approach for Sanfilippo disease. *Eur. J. Hum. Genet.* **18,** 200–205
35. Dziedzic, D., Narajczyk, M., Gabig-Cimińska, M., and Jakóbkiewicz-Banecka, J. (2012) Simultaneous siRNA-mediated silencing of pairs of genes coding for enzymes involved in glycosaminoglycan synthesis. *Acta Biochim. Pol.* **59,** 293–298
36. Arfi, A., Richard, M., Gandolphe, C., and Scherman, D. (2010) Storage correction in cells of patients suffering from mucopolysaccharidoses types IIIA and VII after treatment with genistein and other isoflavones. *J. Inherit Metab. Dis.* **33,** 61–67
37. Palmieri, M., Impey, S., Kang, H., di Ronza, A., Pelz, C., Sardiello, M., and Ballabio, A. (2011) Characterization of the CLEAR network reveals an integrated control of cellular clearance pathways. *Hum. Mol. Genet.* **20,** 3852–3866
38. Medina, D. L., Fraldi, A., Bouche, V., Annunziata, F., Mansueto, G., Spampanato, C., Puri, C., Pignata, A., Martina, J. A., Sardiello, M., Palmieri, M., Polishchuk, R., Puertollano, R., and Ballabio, A. (2011) Transcriptional activation of lysosomal exocytosis promotes cellular clearance. *Dev. Cell* **21,** 421–430
39. Settembre, C., Di Malta, C., Polito, V. A., Garcia Arencibia, M., Vetrini, F., Erdin, S., Erdin, S. U., Huynh, T., Medina, D., Colella, P., Sardiello, M., Rubinsztein, D. C., and Ballabio, A. (2011) TFEB links autophagy to lysosomal biogenesis. *Science* **332,** 1429–1433
40. Sardiello, M., and Ballabio, A. (2009) Lysosomal enhancement: a CLEAR answer to cellular degradative needs. *Cell Cycle* **8,** 4021–4022
41. Morgan, T. M., Koreckij, T. D., and Corey, E. (2009) Targeted therapy for advanced prostate cancer: inhibition of the PI3K/Akt/mTOR pathway. *Curr. Cancer Drug Targets* **9,** 237–249